NACA

RESEARCH MEMORANDUM

PERFORMANCE OF A 20-INCH STEADY-FLOW RAM JET AT HIGH ALTITUDES AND RAM-PRESSURE RATIOS

By Eugene Perchonok, William H. Sterbentz and Fred A. Wilcox

Flight Propulsion Research Laboratory
Cleveland, Ohio

NATIONAL ADVISORY COMMITTEE FOR AERONAUTICS

WASHINGTON

June 25, 1947

NACA RM No. E6L06

NATIONAL ADVISORY COMMITTEE FOR AERONAUTICS

RESEARCH MEMORANDUM

PERFORMANCE OF A 20-INCH STEADY-FLOW RAM JET AT HIGH ALTITUDES AND RAM-PRESSURE RATIOS

By Eugene Perchonok, William H. Sterbentz
and Fred A. Wilcox

SUMMARY

The results of an investigation conducted in the Cleveland altitude wind tunnel to determine the performance of a 20-inch ram jet are presented and discussed. The investigation was conducted at altitudes ranging from 7000 to 41,500 feet and at ram-pressure ratios equivalent to free-stream Mach numbers as great as 1.84 using preheated 62-octane fuel. Supplementary tests to determine any change in performance caused by changing the fuel to preheated 100-octane were also made. An extension of the methods of data reduction and of the generalizing performance parameters applicable at supersonic Mach numbers and over a wide range of operating conditions is presented. The magnitudes of the total-pressure losses across the various phases of the ram-jet cycle are analyzed and discussed.

At an equivalent free-stream Mach number of 1.84 and a gas total-temperature ratio across the engine of 5.7, the equivalent sea-level net thrust was 8135 pounds. For these conditions, the over-all efficiency was 12.6 percent and the combustion efficiency was 70.3 percent. The corresponding net-thrust coefficient was 0.74. The investigation also showed that no change in the performance or operating range of the engine occurred when the fuel was changed from preheated 62-octane to preheated 100-octane gasoline.

INTRODUCTION

Experiments have been conducted at the NACA Cleveland laboratory to determine the feasibility of operating a ram jet at high altitudes and at ram-pressure ratios equivalent to supersonic flight speeds. Performance studies of a ram jet at equivalent free-stream Mach numbers to 1.26 and at altitudes to 30,000 feet were made at this laboratory and are reported in references 1 and 2. Other ram-jet studies (references 3 to 6) present subsonic ram-jet performance.

In the present investigation made to extend the performance data, dry refrigerated air was admitted to a 20-inch ram jet mounted in the altitude wind tunnel. The desired ram-pressure ratio across the engine was obtained by throttling the inlet air to the ram jet from approximately sea-level pressure and adjusting the static pressure in the tunnel. The performance of the engine was studied at altitudes up to 41,500 feet and ram-pressure ratios equivalent to Mach numbers as great as 1.84. The selection of the ram-jet configuration used in this study was based on the results of previous investigations (references 1 and 2).

The results obtained in this investigation are summarized and the effect of a variation in combustion-chamber length on engine performance at high altitudes and at ram-pressure ratios equivalent to supersonic flight speeds is discussed. The development of the parameters by means of which the performance of ram jets can be generalized to any desired operating conditions, originally presented in reference 1, has been amplified to include additional variations encountered in the greater operating range covered in this investigation. In the expression of the values of ram-pressure ratio at which the engine was operated in terms of equivalent free-stream Mach number, the effect of shock losses that would occur at supersonic flight velocities are included.

APPARATUS AND PROCEDURE

The 20-inch ram jet used in the investigation was mounted in the altitude-wind-tunnel test section below a 7-foot chord wing, which was supported at the tips by the wind-tunnel balance frame (fig. 1). Dry refrigerated air was supplied to the ram jet through a pipe from the wind-tunnel make-up air duct. This air was available in the make-up air duct at approximately sea-level pressure and was throttled to provide the desired total pressure at the diffuser inlet. The ram jet exhausted directly into the wind tunnel, in which the pressure altitude was varied to obtain different values of ram-pressure ratio across the unit. Restraint of the model by the ram pipe was obviated by a sealed slip joint inserted between the ram pipe and the diffuser inlet. The tunnel balance system could then be used to measure the thrust.

The diffuser had an 8° included angle, a 14-inch-diameter inlet, and a 20-inch-diameter exit. The engine was operated with replaceable 20-inch-diameter, 5- and 12-foot combustion-chamber sections to which a converging nozzle 2 feet long with a 16.8-inch-diameter exit was attached. The shell was cooled by circulating water through copper tubing wrapped around the combustion chamber and exhaust nozzle.

Two different fuel injector systems (fig. 2) were used with no apparent change in operation of the engine. One system consisted of

four 1/4-inch steel tubes having a total of 68 No. 70 holes drilled along the tube lengths. These holes were equally spaced along the four tubes and extended to within 2 inches of the diffuser wall. The other system consisted of seven steel tubes having the same number and size of holes equally spaced along the tubes. The total of 11 tubes were equally spaced and arranged in an 80° V pattern; the open end of the V was 5 inches downstream of the diffuser inlet. The fuel was injected directly upstream.

A flame holder (fig. 3), consisting of a grid of horizontal and vertical 30° V's 1 inch across the open end and with $2\frac{1}{2}$-inch vertex spacing, was mounted at the combustion-chamber inlet with the vertices of the V's facing upstream. A gas pilot to start combustion was built into the flame holder and ignition for the pilot was provided by a modified aircraft spark plug. The cold static-pressure drop across the flame holder was 2.9 times the dynamic pressure at the combustion-chamber inlet.

The steam heat-exchanger fuel-preheating system described in reference 2 was also used in this investigation. The fuel temperature was maintained at 220° ±40° F by regulating the steam flow. An unleaded 62-octane gasoline (AN-F-22) was used. Supplementary tests were also made using a leaded 100-octane gasoline (AN-F-28).

During operation, local hot spots were observed on the combustion-chamber shell under the copper cooling coils. An experimental section (fig. 4), which eliminated all tendencies toward local overheating, was inserted as part of the combustion chamber. The section was constructed by seam-welding an outer shell corrugated to form a helical cooling-water path to a smooth, cylindrical inner shell.

Static pressures, total pressures, and indicated temperatures were measured with a survey rake mounted at the diffuser inlet. These pressures and temperatures were used to compute the air flow through the engine and the velocities at the diffuser inlet and exit. The fuel flow was determined with a rotameter. Fuel temperatures and pressures were measured at the injector manifold.

Data were obtained at pressure altitudes ranging from 7000 to 41,500 feet. The fuel-air ratio was varied from approximately 0.040 to 0.067. Under choking conditions at the exhaust nozzle (jet Mach number greater than 1), the maximum fuel-air ratio was limited to 0.051 because the peak delivery rate of the fuel pump had been reached and the minimum fuel-air ratio was limited to approximately 0.042 because the fuel-injector pressure dropped below the fuel vapor pressure at this point. The inlet-air temperature was maintained at 10° ±10° F.

[redacted]

SYMBOLS

The following symbols are used in this paper:

A	cross-sectional area, square feet
C_F	net-thrust coefficient, $\frac{2F_n}{\gamma_0 p_0 A_3 M_0^2}$
c_p	specific heat at constant pressure, Btu per pound per $^\circ F$
F_j	jet thrust, pounds
F_n	net thrust, pounds
f/a	fuel-air ratio
g	acceleration of gravity, feet per second per second
h	lower heating value of fuel, 19,000 Btu per pound
J	mechanical equivalent of heat, foot-pounds per Btu
M	Mach number
m_g	mass gas flow, slugs per second
P	total pressure, pounds per square foot absolute
p	static pressure, pounds per square foot absolute
R	gas constant, foot-pound per pound per $^\circ F$
T	total temperature, $^\circ R$
t	static temperature, $^\circ R$
V	velocity, feet per second
W_a	air flow, pounds per second
W_f	fuel flow, pounds per second
γ	ratio of specific heat at constant pressure to specific heat at constant volume

δ	ratio of absolute tunnel ambient pressure to absolute static pressure at NACA standard atmospheric conditions at sea level, $p_0/2116$
θ_4	ratio of absolute total temperature at exhaust-nozzle exit to absolute static temperature at NACA standard atmospheric conditions at sea level, $T_4/519$
η	over-all efficiency, percent
η_b	combustion efficiency, percent
τ_1	ratio of absolute total temperature at exhaust-nozzle exit to absolute total temperature at diffuser inlet, T_4/T_1
τ_2	ratio of absolute total temperature at exhaust-nozzle exit to absolute total temperature at combustion-chamber inlet, T_4/T_2

Subscripts:

0	equivalent free-stream condition
1	station 1, subsonic diffuser inlet
2	station 2, diffuser exit and combustion-chamber inlet
3	station 3, combustion-chamber exit
4	station 4, exhaust-nozzle exit
j	exhaust-jet condition at ambient pressure ($p_j = p_0$)

Performance parameters:

F_j/δ	jet thrust reduced to NACA standard atmospheric conditions at sea level, pounds
F_n/δ	net thrust reduced to NACA standard atmospheric conditions at sea level, pounds
$M_2\sqrt{\tau_2}$	combustion-chamber-inlet Mach number parameter

[redacted]

$\eta(1 + \sqrt{\tau_1})$	over-all efficiency parameter, percent
$\frac{\eta}{\eta_b}(1 + \sqrt{\tau_1})$	ideal over-all efficiency parameter, percent
$\frac{W_a}{\delta}\sqrt{\theta_4}$	air-flow parameter, pounds per second
$\frac{W_f \eta_b \ 3600}{\delta\sqrt{\theta_4}}$	fuel-consumption parameter, pounds per hour
$\frac{550\ W_f\ 3600}{F_n V_0}$	net-power specific fuel consumption, pounds per net thrust horsepower-hour
$\frac{550\ W_f\ 3600}{F_n V_0(1 + \sqrt{\tau_1})}$	net-power specific fuel consumption parameter, pounds per net thrust horsepower-hour
$\frac{550\ W_f\ 3600}{F_n V_0(1 + \sqrt{\tau_1})}\eta_b$	ideal net-power specific fuel consumption parameter, pounds per net thrust horsepower-hour

RESULTS AND DISCUSSION

At all fuel-air ratios at which the engine was operated, flame completely filled the combustion chamber. High-speed motion-picture studies indicated, however, that the burning, which appeared to be smooth but was accompanied by a steady buzzing sound, was actually of a high-frequency pulsating nature.

Below choking (jet Mach number less than 1), the flame emitted from the exhaust nozzle was continuous except for occasional flashes curling outward. Above choking (jet Mach number greater than 1), the operation of the engine seemed independent of tunnel ambient pressure and shock bands were clearly visible in the exposed flame. These shock bands were spaced approximately uniformly along the jet from the nozzle exit. Little flame color could be seen between the nozzle exit and the first bright band (fig. 5). (For an exposition of the aerodynamic characteristics of supersonic gas jets, see reference 7.)

In general, the data for this investigation have been reduced and correlated by methods discussed in reference 1. In certain instances, however, the performance parameters of reference 1 were oversimplified because of the narrow operating range covered and proved inadequate for correlating the data at the high Mach numbers obtained in this investigation. A refinement and an extension of the performance parameters and methods of data reduction applicable to performance at high Mach numbers and over a wide operating range are presented in the appendix.

The equivalent free-stream Mach number M_0 is taken as the independent variable in presenting the data. This quantity is calculated from the equivalent free-stream total pressure and the tunnel ambient static pressure. For values of M_0 less than 1, the diffuser-inlet total pressure was taken as the equivalent free-stream total pressure. For values of M_0 greater than 1, supersonic diffuser losses were added to the measured subsonic diffuser-inlet total pressure to obtain the equivalent free-stream total pressure. The assumptions used in obtaining the equivalent free-stream total pressure and M_0 from the measured diffuser-inlet total pressure and the tunnel ambient static pressure for $M_0 > 1$ are given in the appendix.

The relations of the performance parameters to M_0 for the 5-foot combustion-chamber engine are presented in figures 6 to 20. An investigation using 100-octane gasoline (AN-F-28) showed no change in the performance of the engine as compared with the performance when 62-octane gasoline (AN-F-22) was used. For this reason, no data for the performance study using 100-octane gasoline are presented. With the exception of the combustion-efficiency data, the test points for the 12-foot combustion chamber fell along the curves established for the 5-foot combustion chamber (figs. 6 to 19). Therefore, only the jet-thrust (figs. 6 and 7) and the combustion-efficiency data (fig. 21) for the 12-foot combustion chamber are presented.

The highest equivalent free-stream Mach number for operation with the 5-foot combustion chamber was 1.84. This maximum was set not by an operational limit of the engine but by the pumping capacity of the test apparatus. With the 12-foot combustion chamber, the highest M_0 at which the engine could be operated before blow-out was 1.19.

The maximum jet thrust developed by the engine with the 5-foot combustion chamber, reduced to sea-level conditions F_j/δ (fig. 6) was 14,690 pounds at $M_0 = 1.84$. The actual jet thrusts F_j measured and the altitudes at which these data were obtained are presented in figure 7. The pressure-altitude contours are based on the reduced jet-thrust curve of figure 6.

[redacted]

As was to be expected, both the jet thrust and the net thrust increased sharply with M_0 (figs. 6 to 8). The net-thrust coefficient also increased with M_0 in the range of this investigation (fig. 9). At the highest equivalent free-stream Mach number attained (1.84), the net thrust reduced to sea-level conditions was 8135 pounds (fig. 8). The corresponding net-thrust coefficient C_F was 0.74 (fig. 9). Both the reduced net thrust and the net-thrust coefficient increased with an increase in the total-temperature ratio across the engine.

Equation (10) of the appendix indicates that the ideal over-all efficiency parameter $\frac{\eta}{\eta_b}(1 + \sqrt{\tau_1})$ is a function of only M_0 and a single curve was obtained when this parameter was plotted as a function of M_0 (fig. 10). Likewise, a single curve was obtained by plotting the ideal net-power specific fuel consumption parameter $\frac{550\ W_f\ 3600}{F_n V_0(1 + \sqrt{\tau_1})}\eta_b$ as a function of M_0 (fig. 11). The over-all efficiency parameter $\eta(1 + \sqrt{\tau_1})$ and the net-power specific fuel consumption parameter $\frac{550\ W_f\ 3600}{F_n V_0(1 + \sqrt{\tau_1})}$ are plotted in figures 12 and 13, respectively, as functions of M_0 and combustion efficiency η_b. From these figures the combustion efficiency at which the data were obtained can be easily determined. The combustion-efficiency contours on figures 12 and 13 were determined from the curves of figures 10 and 11, respectively. Figures 12 and 13 can be used to calculate the actual values of engine over-all efficiency and net-power specific fuel consumption. The values of τ_1, which are needed to determine the over-all efficiency and net-power specific fuel consumption, can be obtained from figure 9. For convenience, the actual values of over-all efficiency η and net-power specific fuel consumption $\frac{550\ W_f\ 3600}{F_n V_0}$ are presented as a function of M_0 in figures 14 and 15, respectively. No curves for different values of η_b have been drawn through the data because variations in τ_1 caused the data to scatter.

The over-all efficiency parameters (figs. 10 and 12) and the over-all efficiency (fig. 14) increased rapidly with Mach number. Concurrently, a rapid decrease in the net-power specific fuel consumption parameters (figs. 11 and 13) and the net-power specific fuel consumption (fig. 15) occurred. At $M_0 = 1.84$, a total-temperature ratio across

the engine τ_1 of 5.7, and a combustion efficiency η_b of 70.3 percent, the over-all efficiency η was 12.6 percent (fig. 14). The corresponding net-power specific fuel consumption $\frac{550\ W_f\ 3600}{F_n V_0}$ was 1.06 pounds per net thrust horsepower-hour (fig. 15).

The variation of the ultimate exhaust-jet Mach number M_j with M_0 is shown in figure 16. Choking at the exhaust nozzle begins approximately at $M_0 = 1.16$. Also presented in figure 16 are theoretical curves of M_j as a function of M_0 and total-pressure ratio across the engine P_j/P_0, assuming the ratio of specific heats at the free-stream condition γ_0 and the exhaust-jet condition γ_j equal to 1.4 and 1.3, respectively. These curves are based on equation (13) of the appendix. The correlation of these theoretical curves and the experimental data indicates the magnitude of the total-pressure loss through the engine.

A discussion and evaluation of the various types of pressure loss in a ram jet are given in references 8 and 9. From the figures of reference 8, the magnitude of the total-pressure losses across the various phases of the ram-jet cycle can be estimated. At a typical engine-performance condition of $M_0 = 1.70$, $\tau_1 = 6.0$, and $M_2 = 0.14$, the theoretical total-pressure ratio is 0.93 across the normal shock in a convergent-divergent supersonic diffuser with optimum contraction ratio (reference 8, fig. 2), 0.96 across the flame holder with a cold pressure-drop coefficient of 2.9 (reference 8, fig. 5), and 0.91 across a constant-area combustion chamber as a result of burning (reference 8, fig. 6). Inasmuch as the total-pressure ratio across the engine was 0.75 at $M_0 = 1.70$ (fig. 16), there remains a total-pressure ratio of 0.92 attributable to losses resulting from shell friction, fuel-injector drag, and subsonic diffuser and exhaust-nozzle inefficiency.

It is impossible to reduce the greatest of the total-pressure losses, the loss caused by combustion in a constant-area tube, if maximum thrust coefficients are desired because the ram jet must be operated at high values of τ_1 and M_2. With continued research and development, it should be possible to decrease the total-pressure losses caused by the flame holder and to decrease the fuel-injector drag, the shell friction, and the diffuser and exhaust-nozzle inefficiencies.

The data in figure 16 can be used to extrapolate the performance of the engine to Mach numbers in excess of those at which the engine

was operated because all of the engine losses, except the supersonic diffuser losses, will remain relatively constant for conditions at which $M_j > 1$ (τ_1 and M_2 constant). The decrease in the theoretical total-pressure recovery across the supersonic portion of a converging-diverging diffuser of optimum contraction ratio with an increase in M_0 can be determined from figure 2 of reference 8. By application of these calculated losses to the total-pressure ratio across the engine at $M_j = 1$ (fig. 16), an extrapolated curve of M_j can be obtained from an extension of the pressure-ratio contours on that figure.

If the absolute total-temperature ratio τ_2 and M_0 are assumed for some desired operating condition, then the Mach number at the combustion-chamber entrance M_2 can be estimated from figure 17. In this figure, the combustion-chamber-inlet Mach number parameter $M_2\sqrt{\tau_2}$ was practically independent of M_0 at Mach numbers greater than 1, although choking first occurred at $M_0 = 1.16$.

The air-flow parameter $\frac{W_a}{\delta}\sqrt{\theta_4}$ and the fuel-consumption parameter $\frac{W_f \eta_b}{\delta}\frac{3600}{\sqrt{\theta_4}}$ are plotted as functions of M_0 in figures 18 and 19, respectively. The air-flow and fuel-consumption parameters were not affected by choking at the exhaust nozzle and continued to increase at $M_0 > 1.16$. The fuel-consumption parameter is presented as a function of τ_2 in addition to M_0 to include the effect of the term $\left(1 - \frac{T_2}{T_4}\right)$ of equation (28), reference 1.

Combustion-efficiency data are presented as a function of fuel-air ratio f/a for the 5-foot and 12-foot combustion chambers in figures 20 and 21, respectively. A comparison of these data indicates that lengthening the combustion chamber from 5 to 12 feet improved the combustion efficiency about 10 percent over the fuel-air-ratio range at which the engine was operated. As in reference 2, the heat losses through the ram-jet shell were not included in the calculation of combustion efficiency. If these heat losses were included, the combustion-efficiency values would be approximately 3 percent higher for the engine having the 12-foot combustion chamber and 1 percent higher for the engine with the 5-foot combustion chamber. The numbers opposite each point indicate the values of combustion-chamber-inlet static pressure p_2, combustion-chamber-inlet Mach number M_2, and exhaust-nozzle-outlet static pressure p_0 (ambient static pressure). These variables are the ones thought to influence combustion efficiency if the combustion-chamber-inlet temperature T_2 is constant.

It was difficult to separate quantitatively the effect of each variable on combustion efficiency. As mentioned in references 1 and 2, a decrease in the combustion-chamber static-pressure level or an increase in M_2 usually resulted in a decrease in combustion efficiency. With approximately static sea-level pressure maintained at the combustion-chamber inlet, pressure altitude apparently had no effect on η_b after choking conditions were attained at the exhaust nozzle. No investigation was made of the effect of reduced p_2 on combustion efficiency and blow-out.

The greatest combustion-chamber-inlet velocity V_2 at which the burner was operated with a 5-foot combustion chamber was 152 feet per second. This velocity was measured at a pressure altitude of 27,000 feet when the engine was operating under choking conditions at the exhaust nozzle ($M_0 = 1.33$) and at a total-temperature ratio across the combustion chamber $T_2 = 5.0$. Blow-out did not occur at this condition and it should not be considered as the limiting combustion-chamber-inlet velocity for this burner. The maximum V_2 attained with a 12-foot combustion chamber was 140 feet per second at a pressure altitude of 23,000 feet. This value was obtained when the engine was operating under choking conditions at the exhaust nozzle ($M_0 = 1.19$).

SUMMARY OF RESULTS

From an investigation of the performance of a 20-inch ram jet over a wide range of pressure altitudes and equivalent free-stream Mach numbers, the following results were observed:

1. A net thrust of 8135 pounds reduced to standard sea-level conditions, a net-thrust coefficient of 0.74, and an over-all efficiency of 12.6 percent were attained at the maximum equivalent free-stream Mach number of 1.84 at which the engine with a 5-foot combustion chamber was operated. The corresponding specific fuel consumption was 1.06 pounds per net thrust horsepower-hour. At this condition the total-temperature ratio across the engine was 5.7 and the combustion efficiency was 70.3 percent.

2. The engine with a 5-foot combustion chamber was operated at combustion-chamber-inlet velocities up to 152 feet per second. This velocity was attained during choking at the exhaust nozzle and at a ratio of absolute total temperature at the exhaust-nozzle exit to that at the combustion-chamber inlet of 5.0.

[redacted]

3. In the range investigated the principal total-pressure loss was caused by combustion. At an equivalent free-stream Mach number of 1.70, a combustion-chamber-inlet Mach number of 0.14, and at a total-temperature ratio across the engine of 6.0, the total-pressure ratio across the engine was 0.75. For these conditions the estimated total-pressure ratios across the various phases of the ram-jet cycle that contribute to total-pressure losses were as follows:

Total-pressure ratio across the supersonic portion of diffuser	0.93
Total-pressure ratio across flame holder	0.96
Total-pressure ratio across combustion chamber as a result of combustion	0.91
Total-pressure ratio caused by losses across subsonic portion of diffuser, exhaust nozzle, fuel injector, and combustion chamber as a result of shell friction	0.92

4. At a constant gas total-temperature ratio across the engine and a constant combustion efficiency, the performance curves of the engine were not noticeably affected by changes in the combustion-chamber length. Although increasing the combustion-chamber length from 5 to 12 feet improved the combustion efficiency, the operating range of the engine was reduced.

5. No change in the performance or operating range of the engine was observed when the fuel was changed from preheated unleaded 62-octane to preheated leaded 100-octance gasoline.

Flight Propulsion Research Laboratory,
National Advisory Committee for Aeronautics,
Cleveland, Ohio.

[redacted]

APPENDIX - METHODS OF DATA REDUCTION

The data presented in this paper have been reduced and correlated for the most part by the methods discussed in reference 1. Because some of the data were obtained at equivalent free-stream Mach numbers M_0 markedly greater than those in reference 1, the methods of data reduction have been modified to include the effects of variables that are negligible at the lower equivalent free-stream Mach numbers.

Equivalent Free-Stream Mach Number

The equivalent free-stream Mach number M_0 was determined from the relation

$$M_0^2 = \frac{2}{\gamma_0 - 1}\left[\left(\frac{P_0}{p_0}\right)^{\frac{\gamma_0-1}{\gamma_0}} - 1\right] \qquad (1)$$

For values of M_0 less than 1, the diffuser-inlet total pressure P_1 was taken as the free-stream total pressure P_0.

For values of M_0 greater than 1, the measured inlet total pressure was adjusted in the ratio of the total pressures across an assumed supersonic diffuser. This pressure ratio was taken as the theoretical pressure ratio across a normal shock at the throat of a convergent-divergent supersonic diffuser designed to allow shock entrance at the pertinent Mach number. (See reference 10.) Because even more favorable pressure ratios have been obtained on a different type of supersonic diffuser (references 11 to 13), this assumption seemed reasonable.

Exhaust-Nozzle-Exit Temperature

As derived in reference 1, the exhaust-nozzle-exit temperature T_4 was determined from the expression

$$T_4 = \frac{p_4 A_4 F_j}{gRm_g^2} - \frac{p_4 A_4^2 (p_4 - p_0)}{gRm_g^2} + \frac{\left[F_j - A_4(p_4 - p_0)\right]^2}{2gJc_{p,4}m_g^2} \qquad (2)$$

When the ultimate exhaust-jet Mach number M_j is less than 1, an error in T_4 of less than 2 percent results if p_4 is assumed equal to p_0.

This assumption, however, leads to increasingly erroneous values of T_4 for conditions of M_j greater than 1. It is necessary to determine p_4 more accurately at the conditions for which M_j is greater than 1.

Because M_4 is approximately equal to 1 for all conditions of M_j greater than 1

$$\frac{P_4}{p_4} = \left(\frac{\gamma_4 + 1}{2}\right)^{\frac{\gamma_4}{\gamma_4 - 1}} \tag{3}$$

Further, the jet thrust F_j can be expressed as

$$F_j = \frac{2\gamma_4}{\gamma_4 - 1} p_4 A_4 \left[\left(\frac{P_4}{p_4}\right)^{\frac{\gamma_4 - 1}{\gamma_4}} - 1\right] + A_4(p_4 - p_0) \tag{4}$$

From a combination of equations (3) and (4), the following expression results:

$$p_4 = \frac{F_j}{A_4(\gamma_4 + 1)} + \frac{p_0}{(\gamma_4 + 1)} \tag{5}$$

Equation (5) was used to determine p_4 for all data presented for conditions where M_j was greater than 1.

Over-All Efficiency Parameter

The over-all efficiency parameter was modified to include the effect of variations in the total-temperature ratio across the engine τ_1 (τ_2 assumed equal to τ_1) on the over-all efficiency. This effect became noticeable at high values of M_0. The over-all efficiency of the engine is

$$\eta = \frac{\text{output}}{\text{input}} = \frac{F_n V_0}{W_f h J} \tag{6}$$

[redacted]

It is assumed that the ratio of specific heats γ does not change through the ram jet, that no energy loss occurs in the diffusion and effusion processes, and that the gas flow is essentially the air flow. Then the net thrust F_n, free-stream velocity V_0, and fuel consumption W_f can be stated as follows:

$$F_n = \frac{W_a}{g} V_0 \left(\sqrt{\tau_1} - 1\right) \tag{7}$$

$$V_0 = \frac{M_0 \sqrt{\gamma_0 g R T_1}}{\sqrt{1 + \frac{\gamma_0 - 1}{2} M_0^2}} \tag{8}$$

$$W_f = \frac{W_a c_{p,0} (T_4 - T_1)}{h \eta_b} \tag{9}$$

Substitution of equations (7), (8), and (9) into equation (6) gives, as an approximation, the over-all efficiency in terms of M_0, η_b, and τ_1. Thus

$$\eta = \frac{(\gamma_0 - 1) M_0^2}{1 + \frac{\gamma_0 - 1}{2} M_0^2} \left(\frac{\eta_b}{1 + \sqrt{\tau_1}}\right) \tag{10}$$

Equation (10) shows that the quantity of $\eta(1 + \sqrt{\tau_1})$ is primarily a function of M_0 and η_b. The quantity $\eta(1 + \sqrt{\tau_1})$ was therefore plotted as a function of M_0 and η_b.

Similarly, by substitution of equation (10) into equation (6), the net-power specific fuel consumption parameter $\frac{550 W_f 3600}{F_n V_0 (1 + \sqrt{\tau_1})}$ is primarily also a function of M_0 and η_b. This quantity was therefore plotted as a function of M_0 and η_b.

Ultimate Exhaust-Jet Mach Number

For conditions at which the ultimate exhaust-jet Mach number M_j was less than 1, its value was calculated by the method described in reference 1. For values greater than 1, M_j was calculated in the following manner:

Because there is relatively small loss in total pressure between stations 4 and j, jet Mach number M_j can be expressed as

$$M_j^2 = \frac{2}{\gamma_j - 1}\left[\left(\frac{P_4}{p_0}\right)^{\frac{\gamma_j - 1}{\gamma_j}} - 1\right] \tag{11}$$

Inasmuch as M_4 is approximately equal to 1.0 for all conditions of M_j greater than 1, P_4 from equation (3) can be substituted into equation (11). Thus, assuming γ_j equal to γ_4

$$M_j^2 = \frac{2}{\gamma_j - 1}\left[\frac{\gamma_j + 1}{2}\left(\frac{p_4}{p_0}\right)^{\frac{\gamma_j - 1}{\gamma_j}} - 1\right] \tag{12}$$

The exhaust-nozzle-exit static pressure p_4 is given by equation (5).

Total-Pressure Ratio Across Engine

The theoretical curves of M_j as a function of M_0 and the total-pressure ratio across the engine P_j/P_0 presented in figure 16 were calculated by means of the following expression:

$$\frac{P_j}{P_0} = \frac{\left[1 + \frac{\gamma_j - 1}{2} M_j^2\right]^{\frac{\gamma_j}{\gamma_j - 1}}}{\left[1 + \frac{\gamma_0 - 1}{2} M_0^2\right]^{\frac{\gamma_0}{\gamma_0 - 1}}} \tag{13}$$

Equation (13) is based on the assumption that p_j is equal to p_0.

REFERENCES

1. Perchonok, Eugene, Wilcox, Fred A., and Sterbentz, William H.: Preliminary Development and Performance Investigation of a 20-Inch Steady-Flow Ram Jet. NACA ACR No. E6D05, 1946.

2. Perchonok, Eugene, Wilcox, Fred A., and Sterbentz, William H.: Investigation of the Performance of a 20-Inch Ram Jet Using Preheated Fuel. NACA RM No. E6I23, 1946.

3. Peterson, C., and DeVault, R. T.: Subsonic Ram Jet Development of the Marquardt Aircraft Co. C-20-.85 Ram Jet Engine. (Summary Report) USCAL Rep. No. 2, Univ. Southern Calif., Dec. 1, 1945. (Revised, March 15, 1946.)

4. Bevans, R. S., Shipman, J. J., Smith, F. W., and Williams, G. C.: Subsonic Ram Jet Combustion Chamber Program. (Summary Report) DIC 6201, Jet Propulsion Combustion Chamber Res., M.I.T., April 16, 1945.

5. Pabst: Vorläufige Aitteilung über den Versuch un der FW-Heizdüse im Windkanal A9 der LFA Braunschweig. Bericht Nr. 09 045, Gasdynamische Versuchsanstalt, Focke-Wulf Flugeugbau G.m.b.H. (Bremen), 1944 (approx.).

6. Sänger, E., and Bredt, I.: Über einen Lorinantriev für Strahljäger. Deutsche Forschungsanstalt für Segelflug E.V., "Ernst Udet", z. Zt. Ainring, Deutsche Luftfahrtforschung, Untersuchungen und Mitteilungen Nr. 3509, ZWB (Berlin-Adlershof), Oct. 1943.

7. Anon.: Supersonic Flow and Shock Waves. A Manual on the Mathematical Theory of Non-Linear Wave Motion. AMP Rep. 38.2R, AMG-NYU No. 62, New York Univ., Appl. Math. Group, NDRC, Appl. Math. Panel, Aug. 1944.

8. Silverstein, Abe: Internal Aerodynamics of Ram Jets. Papers presented before the NACA Conference on Supersonic Aerodynamics (Ames Aero. Lab.), June 4, 1946.

9. Williams, Glenn C., and Quinn, John C.: Ram Jet Power Plants. OSRD, Jet-Propelled Missiles Panel, Coordinator Res. and Development, U.S. Navy (Washington, D.C.), May 1945.

10. Kantrowitz, Arthur, and Donaldson, Coleman duP.: Preliminary Investigation of Supersonic Diffusers. NACA ACR No. L5D20, 1945.

11. Oswatitsch, Kl.: Der Druckrückgewinn bei Geschossen mit Rückstossantrieb bei hohen Überschallgeschwindigkeiten (Der Wirkungsgrad von Stossdiffusoren). Bericht Nr. 1005, Forschungen und Entwicklungen des Heereswaffenamtes, Kaiser Wilhelm-Inst. f. Strömungsforschung, Göttingen, Jan. 1944. (The Pressure Recovery of Projectiles with Jet Propulsion at High Supersonic Speeds (The Efficiency of Thrust Diffusors). Trans. by Douglas Aircraft Co., Inc., 1946.)

12. Oswatitsch, Kl., and Böhm, H.: Luftkräfte und Strömungsvorgänge bei angetriebenen Geschossen. Bericht Nr. 1010, Nr. 1010/2, Forschungen und Entwicklungen des Heereswaffenamtes, Kaiser Wilhelm-Inst. f. Strömungsforschung, Göttingen, Aug., Oct. 1944. (Air Forces and Flow Phenomena on Propelled Projectiles.) Trans. by Douglas Aircraft Co., Inc., Feb. 14, 1946.)

13. Moeckel, W. E., Connors, J. F., and Schroeder, A. H.: Investigation of Shock Diffusers at Mach Number 1.85. I - Projecting Single-Shock Cones. NACA RM No. E6K27, 1947.

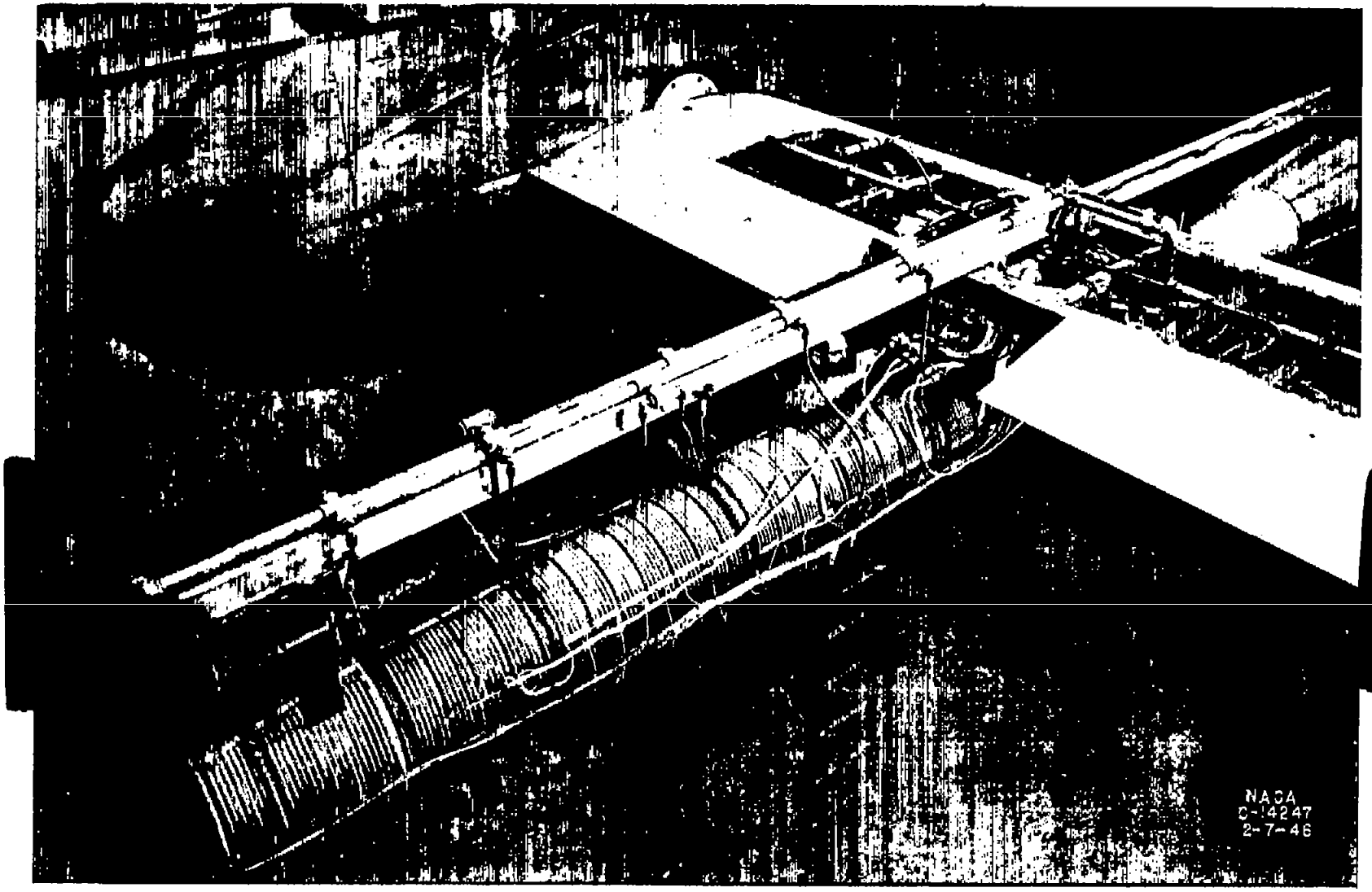

Figure 1.-Installation of 20-inch ram jet with 12-foot combustion chamber and 16.8-inch-diameter exhaust nozzle in altitude wind tunnel.

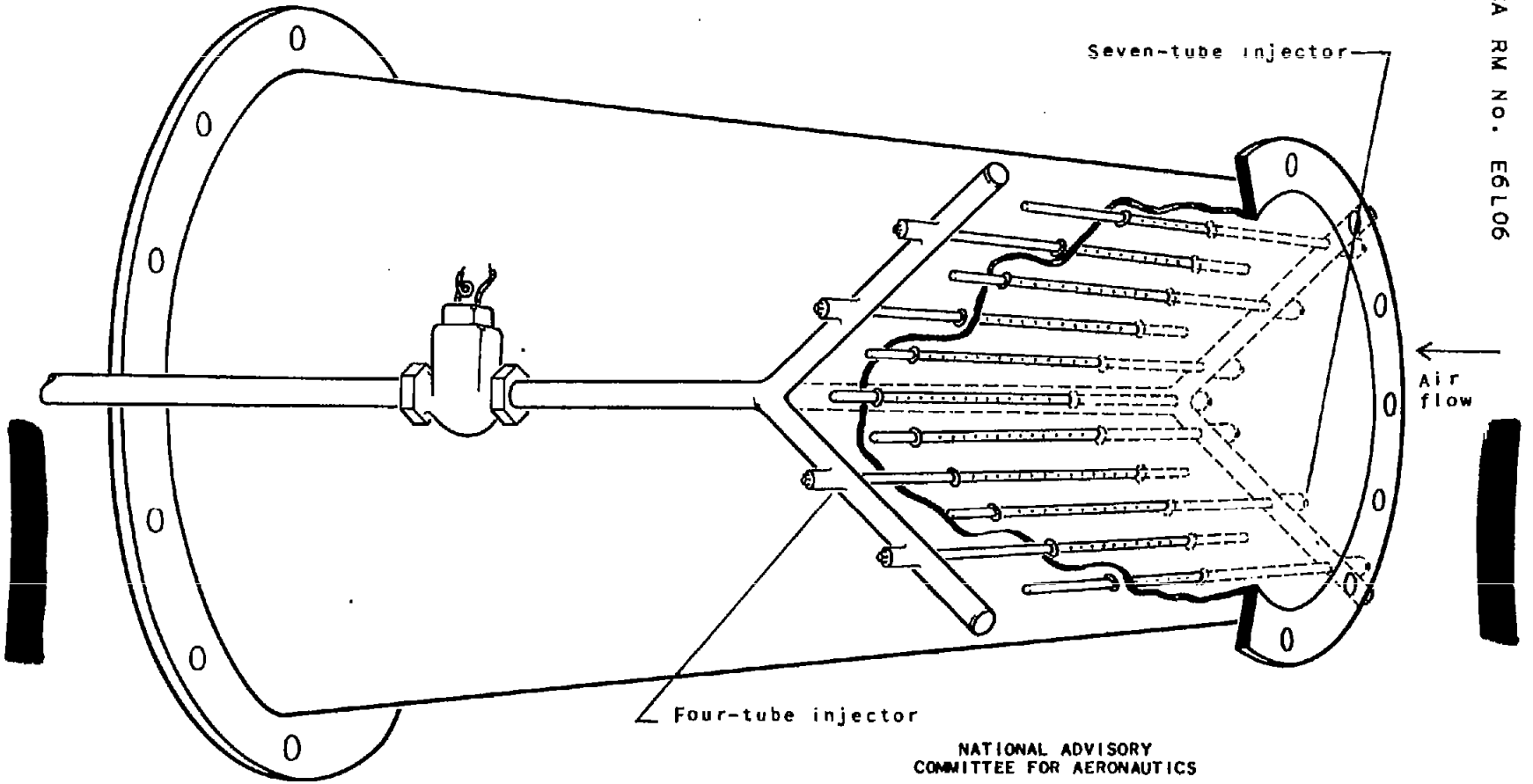

Figure 2. - Installation of four- and seven-tube fuel injectors in 20-inch ram-jet diffuser.

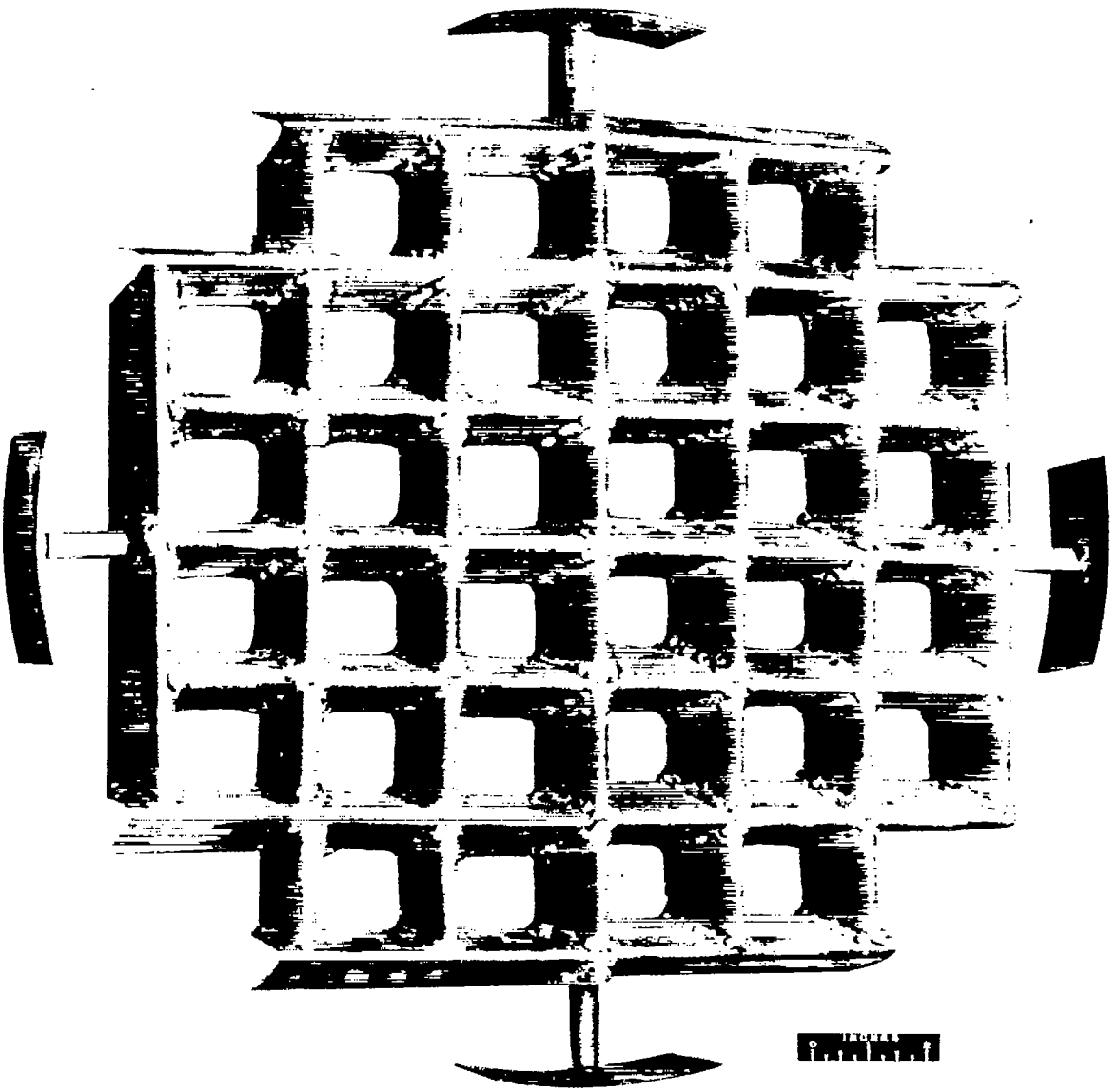

Figure 3. - Flame holder used in wind-tunnel investigation of 20-inch ram jet.

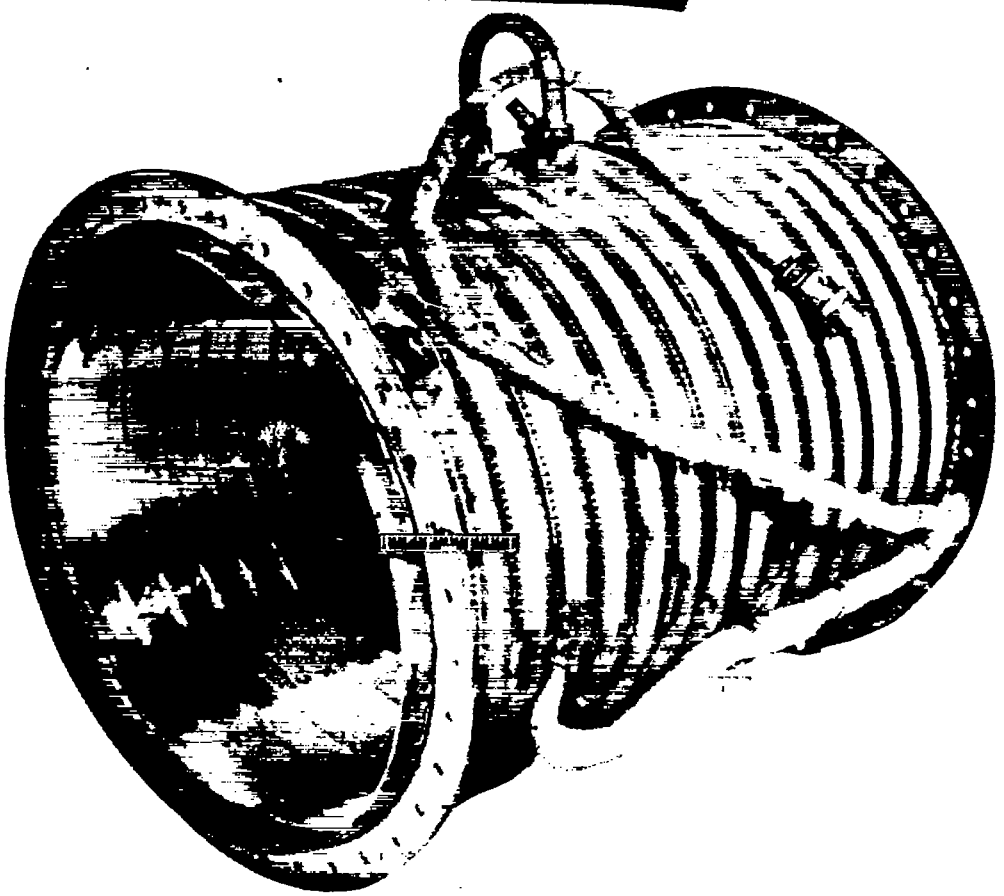

Figure 4. - Modified combustion-chamber section used in wind-tunnel investigation of 20-inch ram jet.

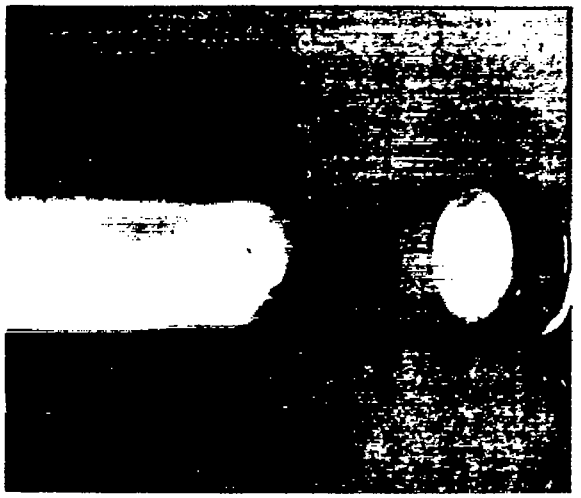

NACA
C-17166
11-13-46

Figure 5. - Exhaust jet issuing at supersonic speeds from exhaust nozzle of 20-inch ram jet during wind-tunnel investigation.

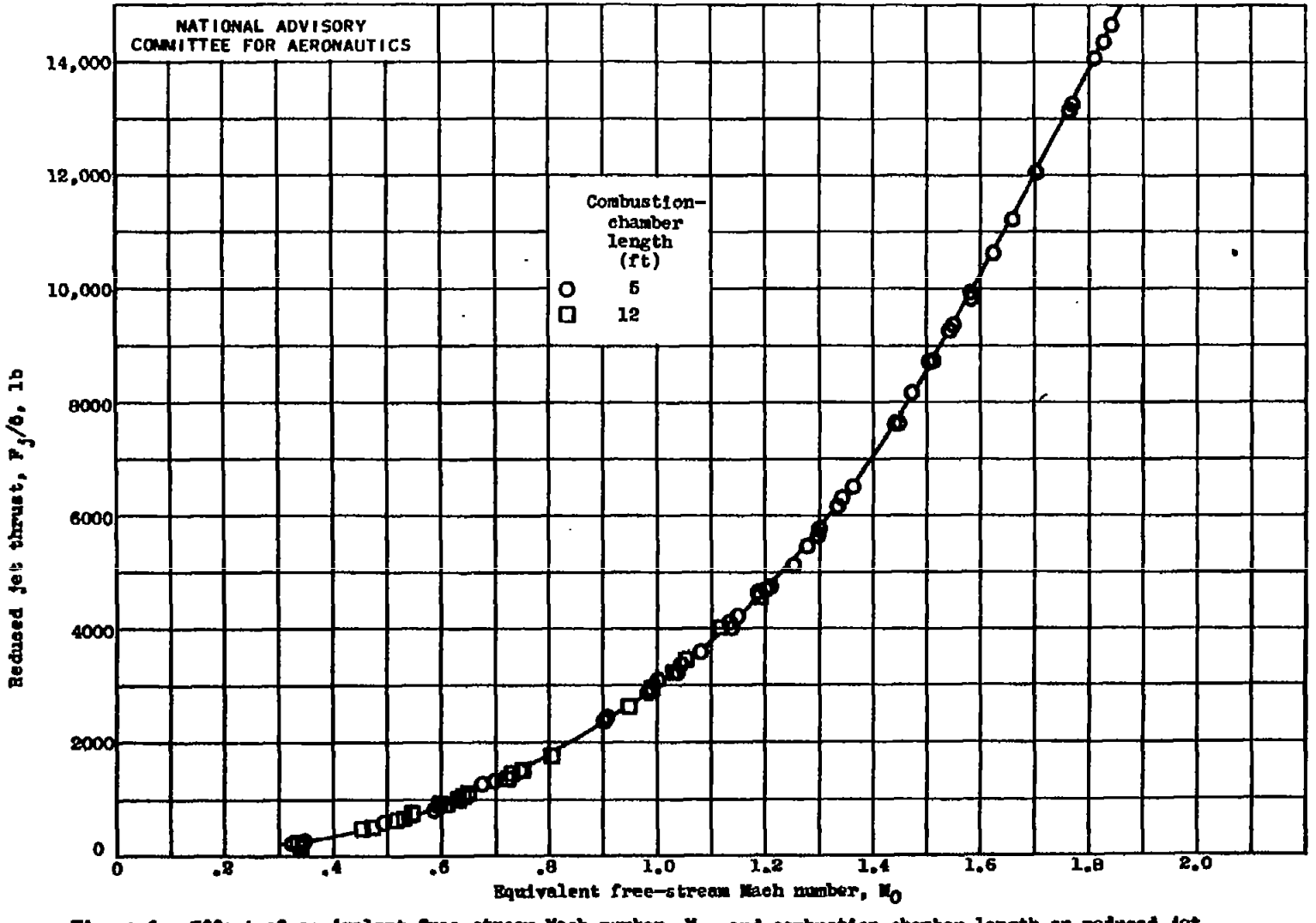

Figure 6.- Effect of equivalent free-stream Mach number M_0 and combustion-chamber length on reduced jet thrust F_j/δ. 20-inch ram jet with 16.8-inch-diameter exhaust nozzle; jet thrust reduced to NACA standard atmospheric conditions at sea level.

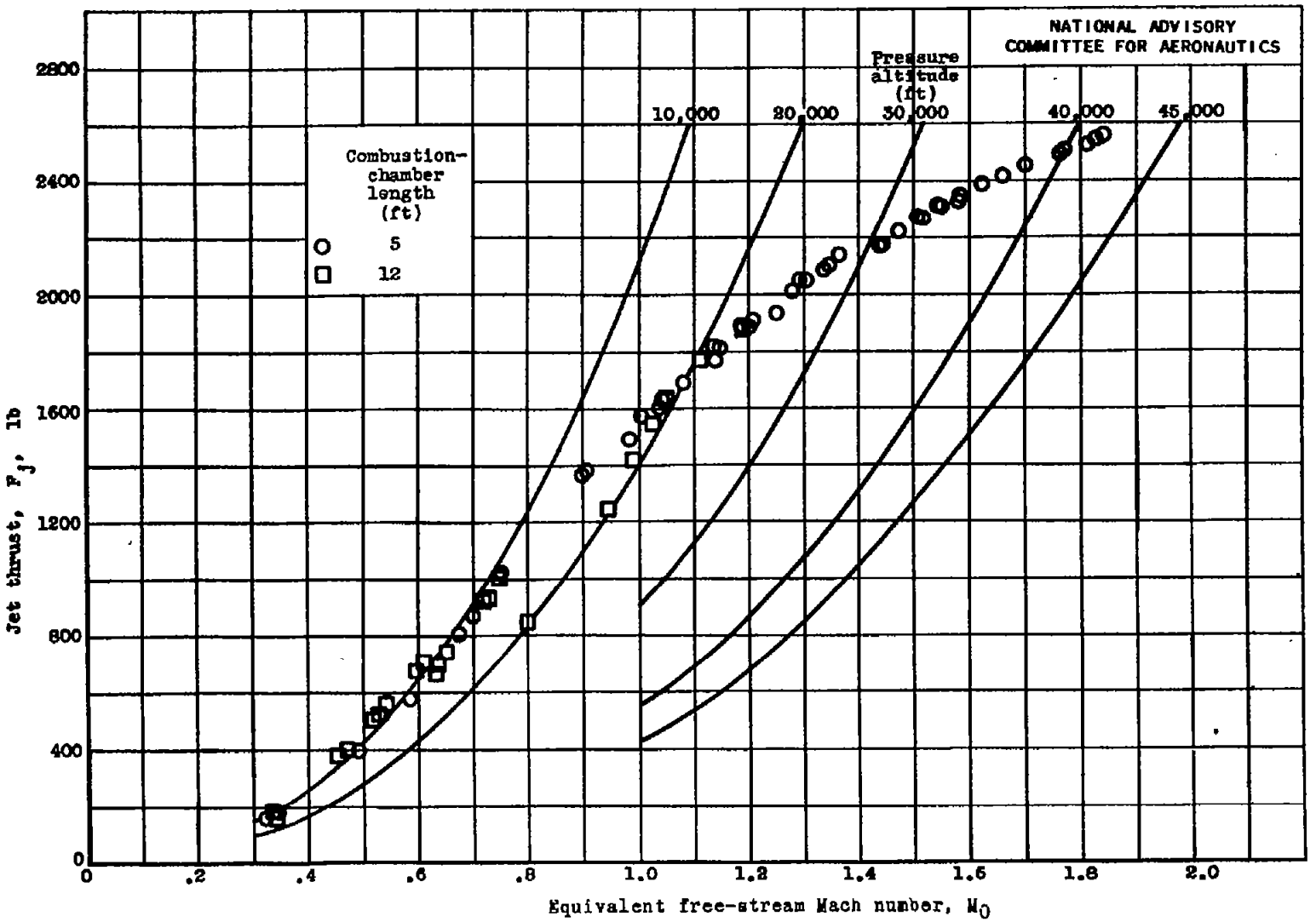

Figure 7.- Effect of equivalent free-stream Mach number M_0, combustion-chamber length, and pressure altitude on jet thrust F_j. 20-inch ram jet with 16.8-inch-diameter exhaust nozzle.

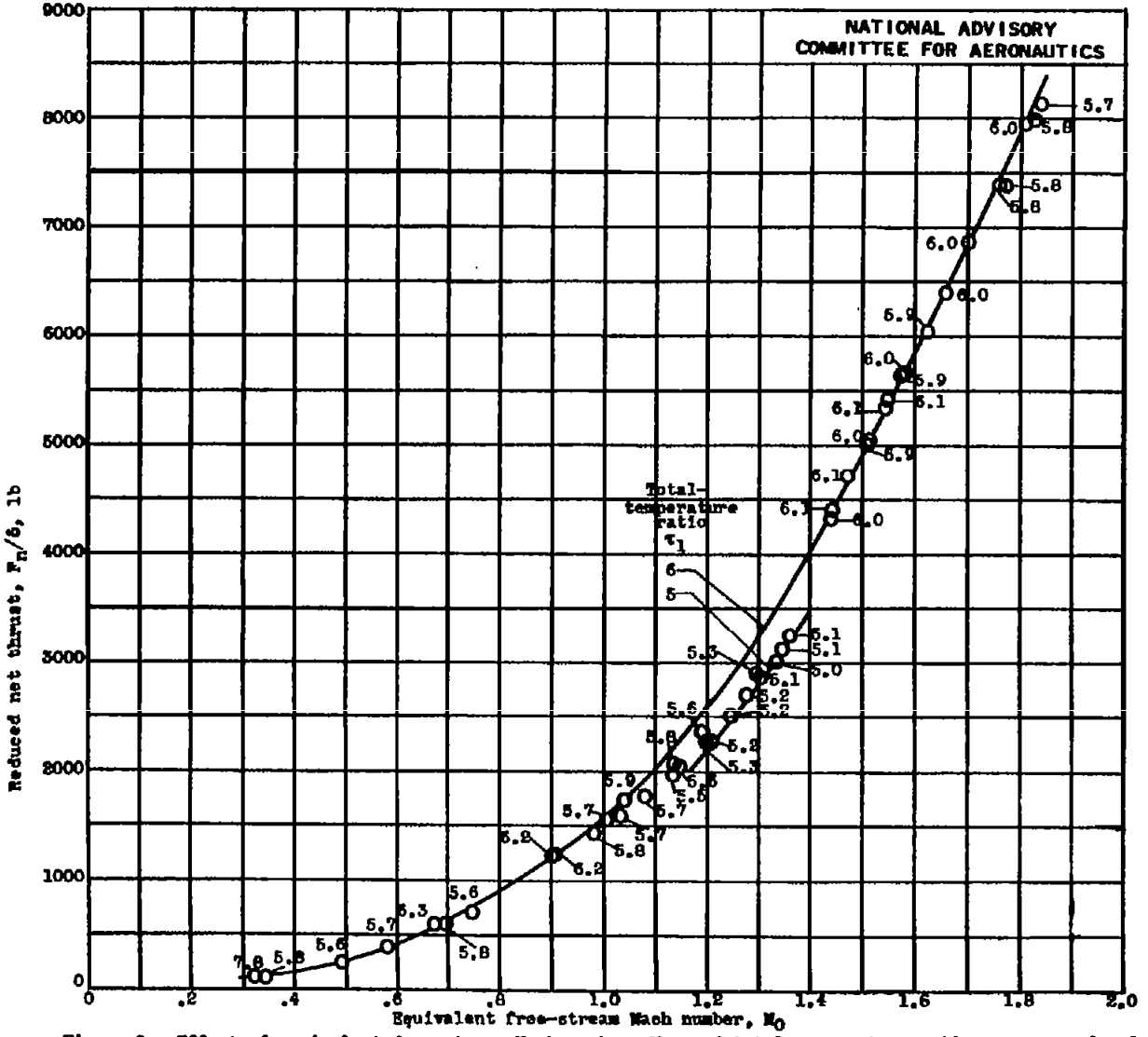

Figure 8.- Effect of equivalent free-stream Mach number M_0 and total-temperature ratio τ_1 on reduced net thrust F_n/δ. 20-inch ram jet with 5-foot combustion chamber and 16.8-inch-diameter exhaust nozzle; net thrust reduced to NACA standard atmospheric conditions at sea level.

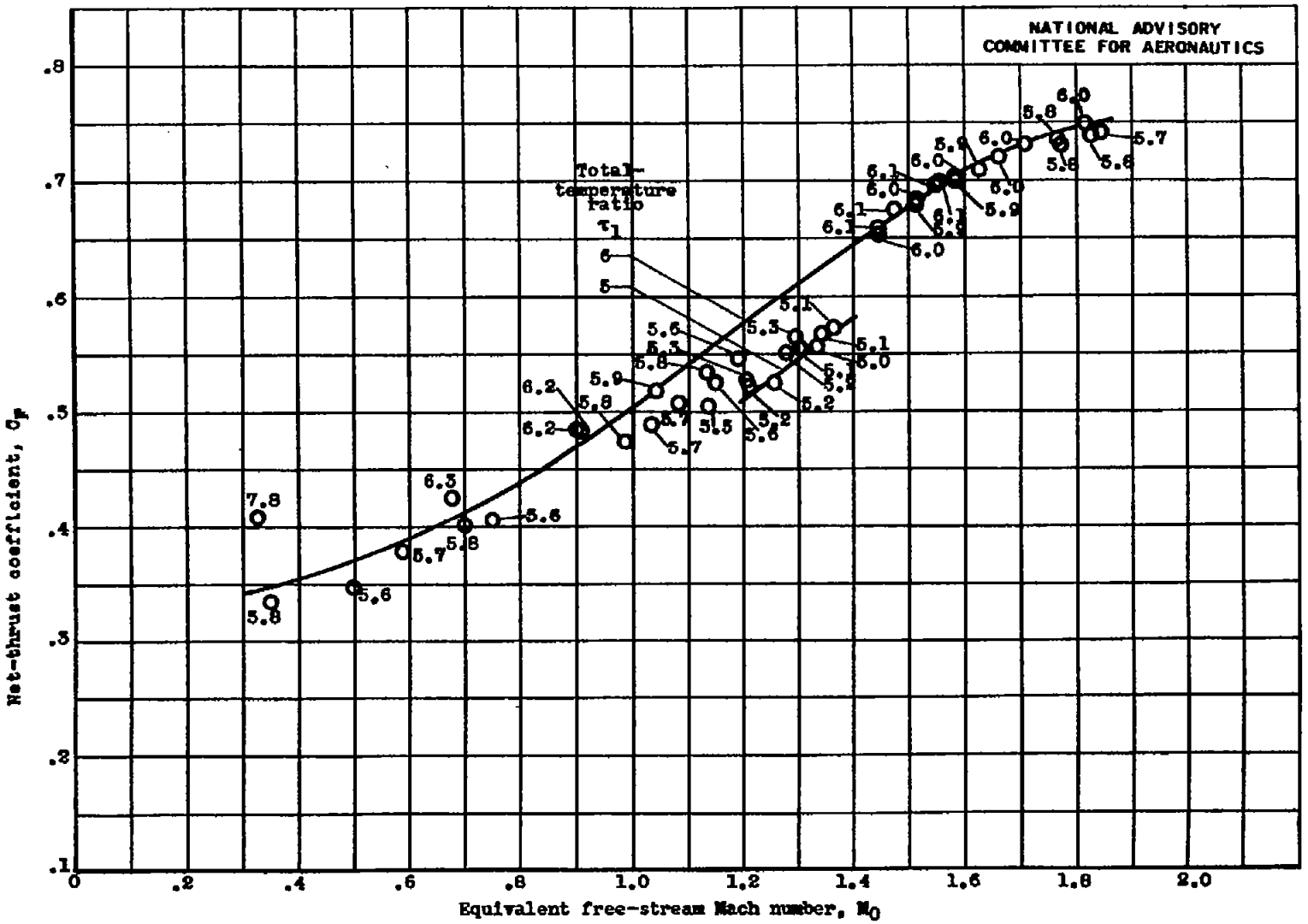

Figure 9.- Effect of equivalent free-stream Mach number M_0 and total-temperature ratio τ_1 on net-thrust coefficient C_F. 20-inch ram jet with 5-foot combustion chamber and 16.8-inch-diameter exhaust nozzle.

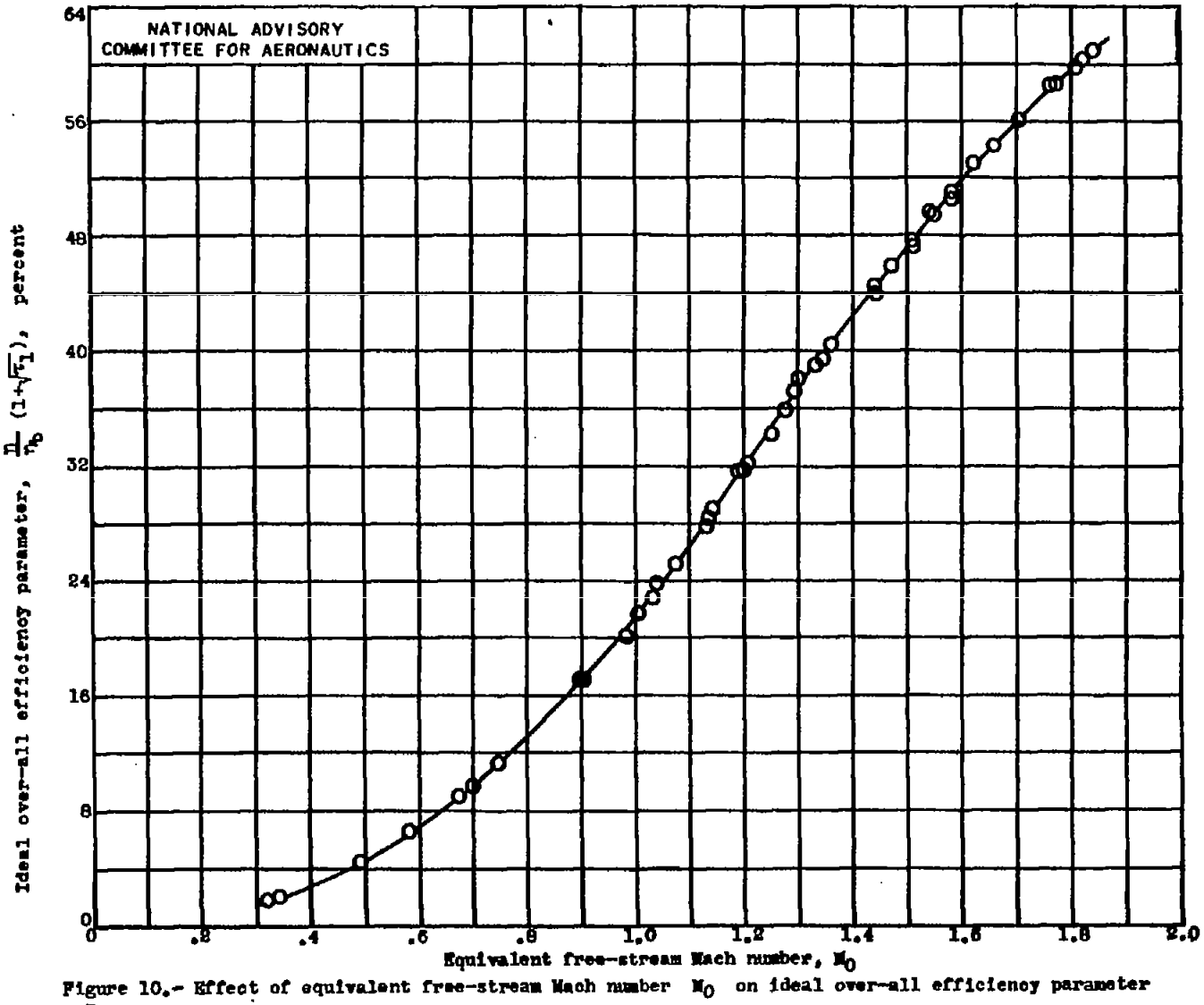

Figure 10.- Effect of equivalent free-stream Mach number M_0 on ideal over-all efficiency parameter $\frac{\eta}{\eta_b}(1+\sqrt{\tau_1})$. 20-inch ram jet with 5-foot combustion chamber and 16.8-inch-diameter exhaust nozzle.

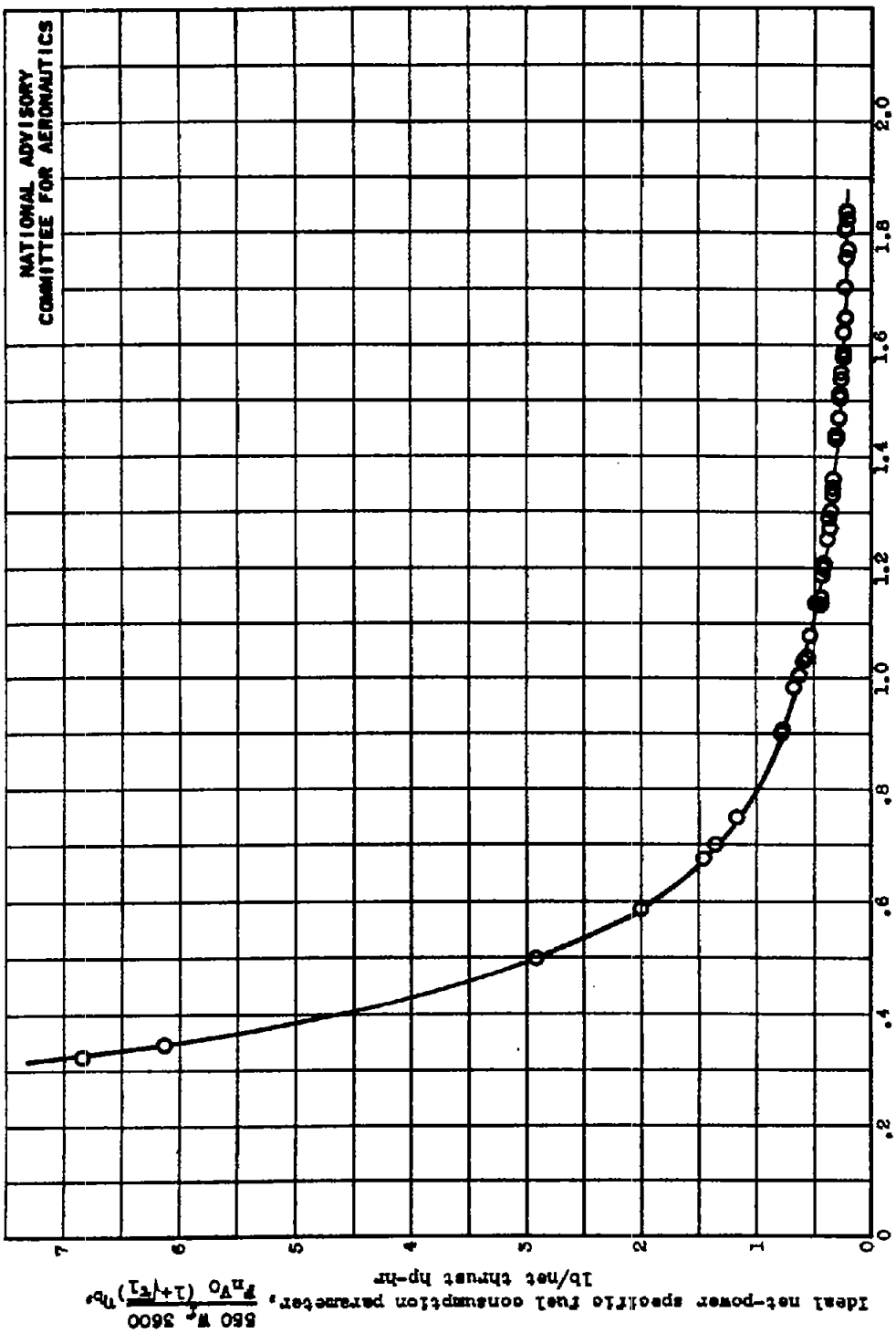

Figure 11.- Effect of equivalent free-stream Mach number M_0 on ideal net-power specific fuel consumption parameter $\frac{550\ W_f\ 3600}{F_n V_0 (1+\sqrt{\tau_1})} \eta_b$. 20-inch ram jet with 5-foot combustion chamber and 16.8-inch-diameter exhaust nozzle.

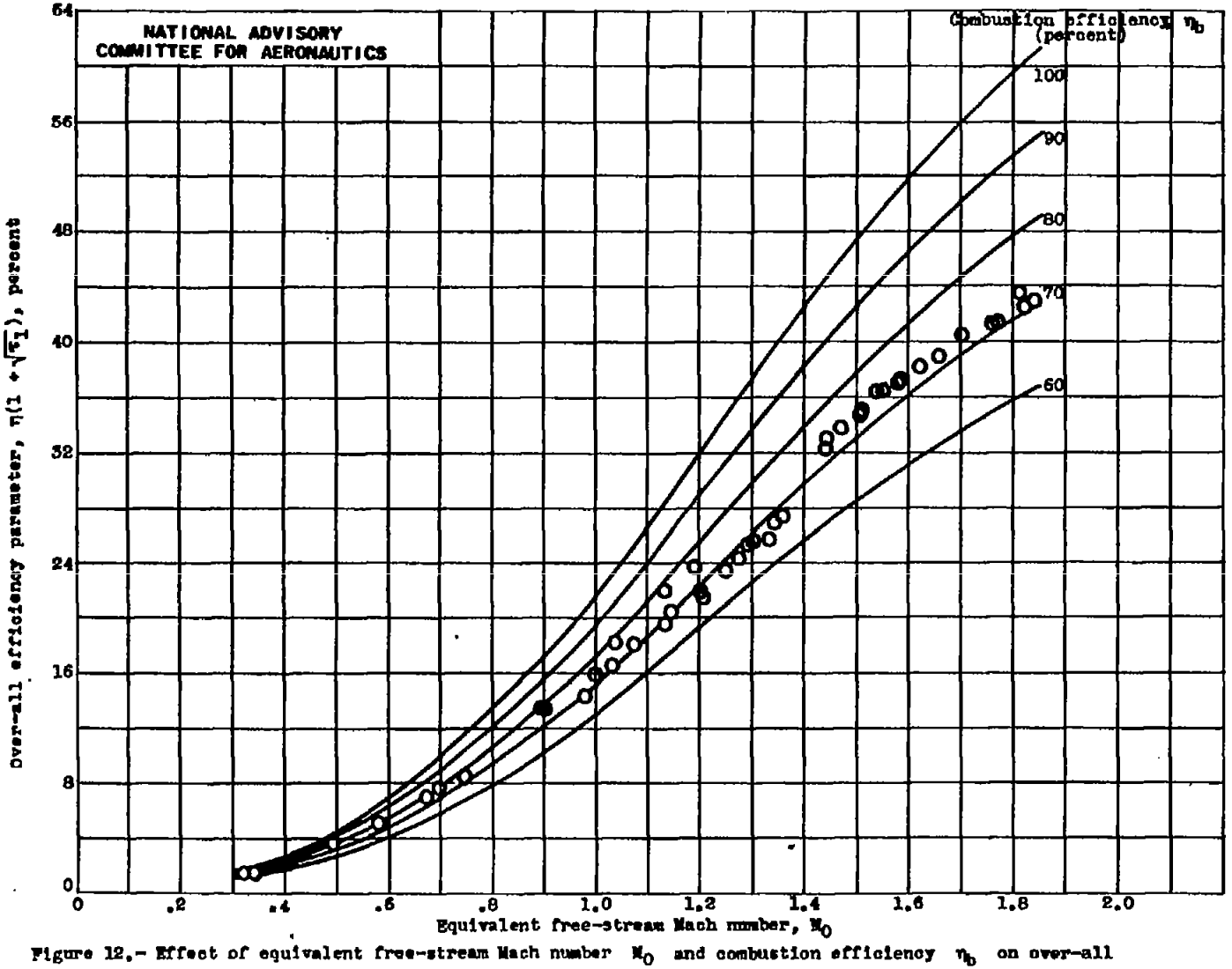

Figure 12.- Effect of equivalent free-stream Mach number M_0 and combustion efficiency η_b on over-all efficiency parameter $\eta(1+\sqrt{\tau_1})$. 20-inch ram jet with 5-foot combustion chamber and 16.8-inch-diameter exhaust nozzle.

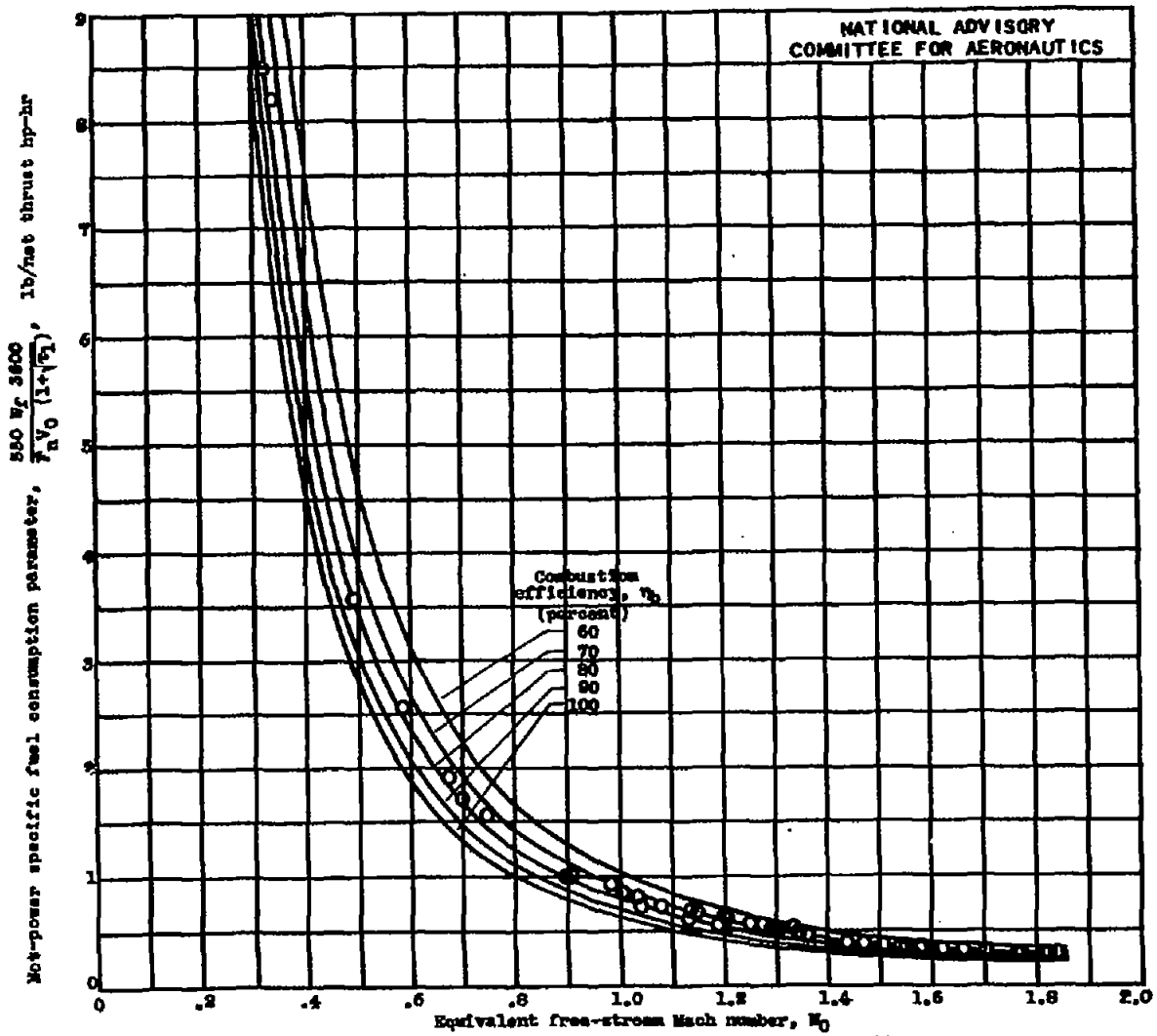

Figure 13.- Effect of equivalent free-stream Mach number M_0 and combustion efficiency η_b on net-power specific fuel consumption parameter $\frac{550\ W_f\ 3600}{F_n V_0\ (1+\sqrt{\tau_1})}$. 20-inch ram jet with 5-foot combustion chamber and 16.8-inch-diameter exhaust nozzle.

CONFIDENTIAL

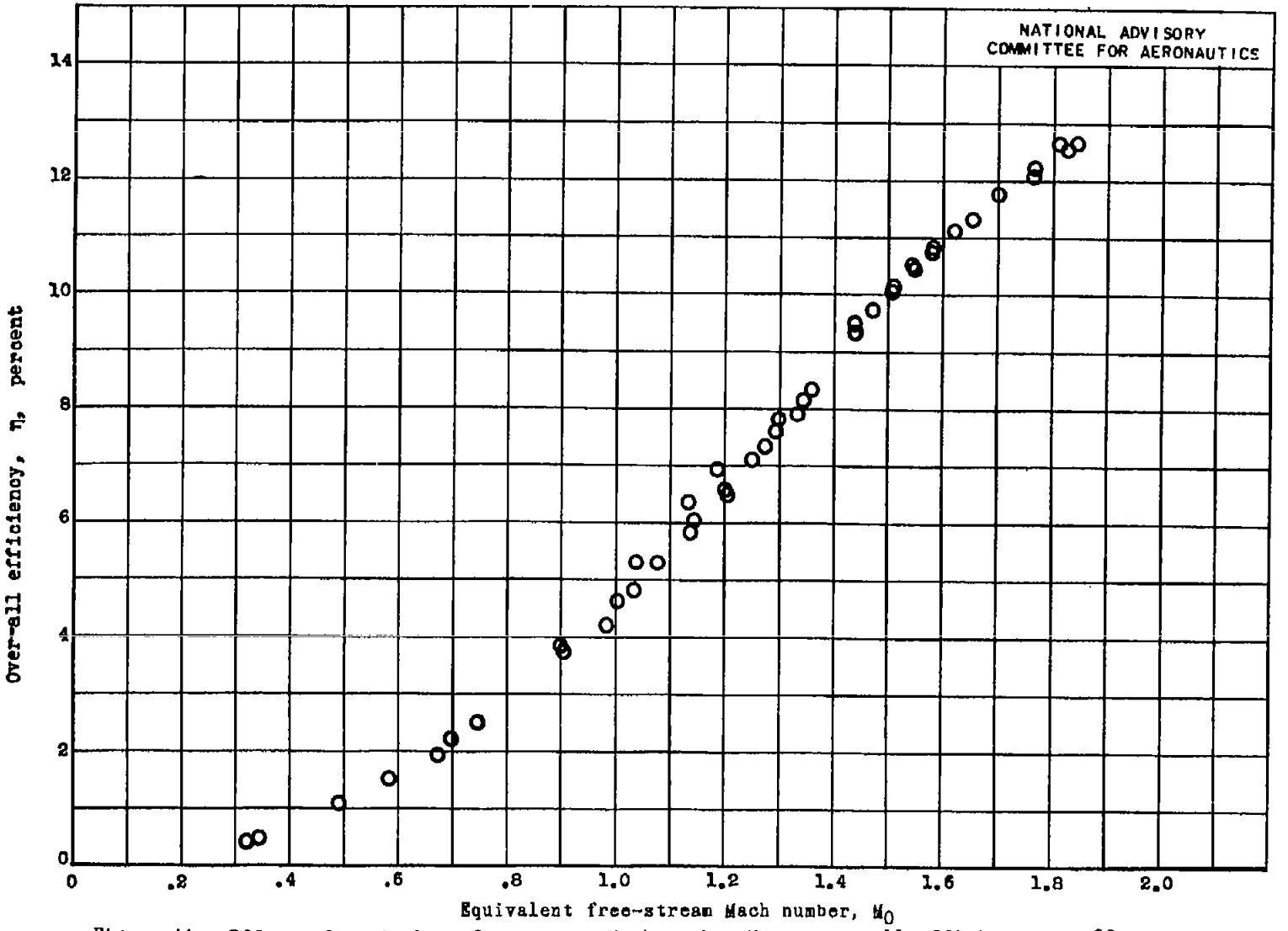

Figure 14.- Effect of equivalent free-stream Mach number M_0 on over-all efficiency η. 20-inch ram jet with 5-foot combustion chamber and 16.8-inch-diameter exhaust nozzle.

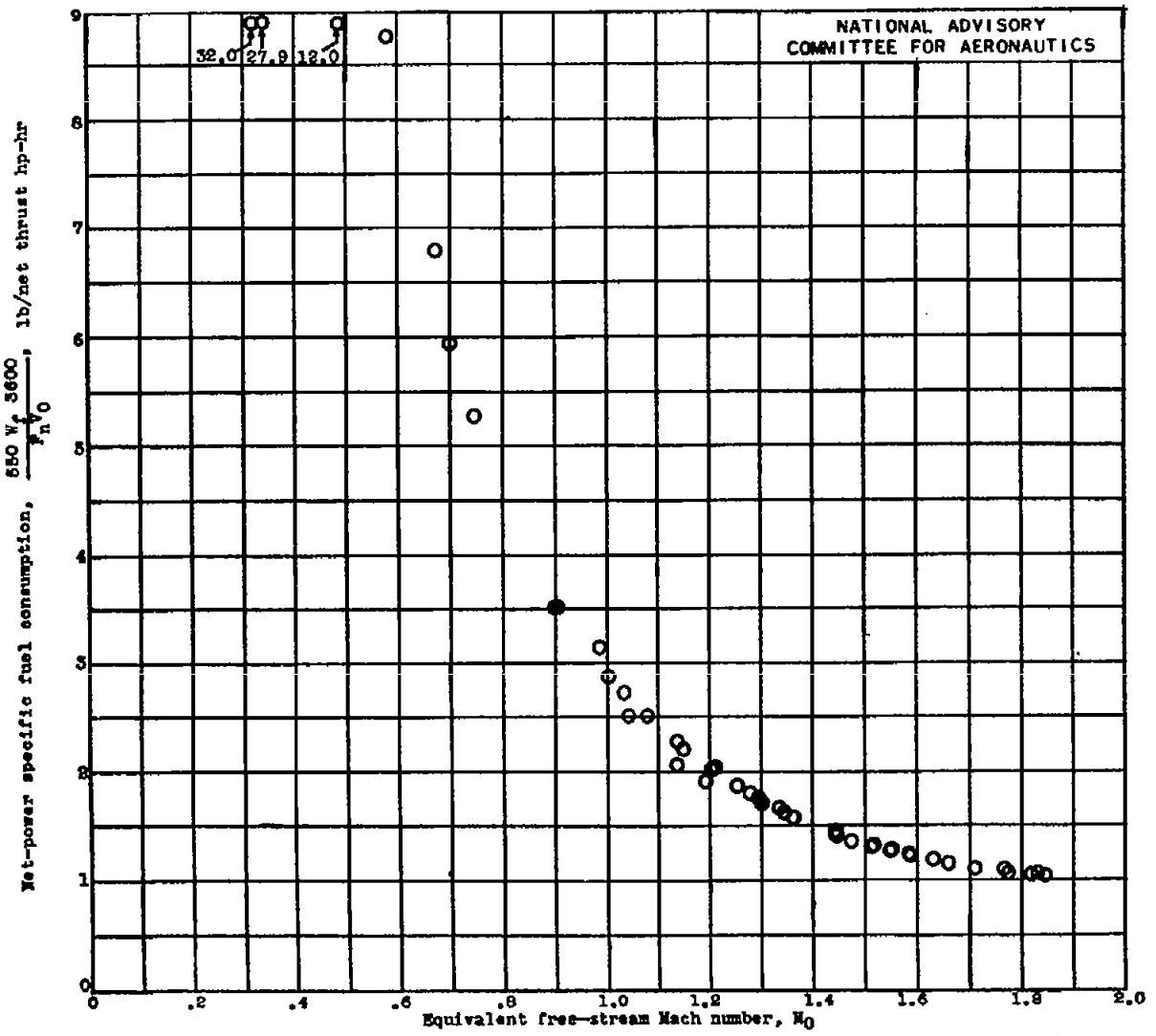

Figure 15.- Effect of equivalent free-stream Mach number M_0 on net-power specific fuel consumption $\frac{550\ W_f\ 3600}{F_n V_0}$. 20-inch ram jet with 5-foot combustion chamber and 16.8-inch-diameter exhaust nozzle.

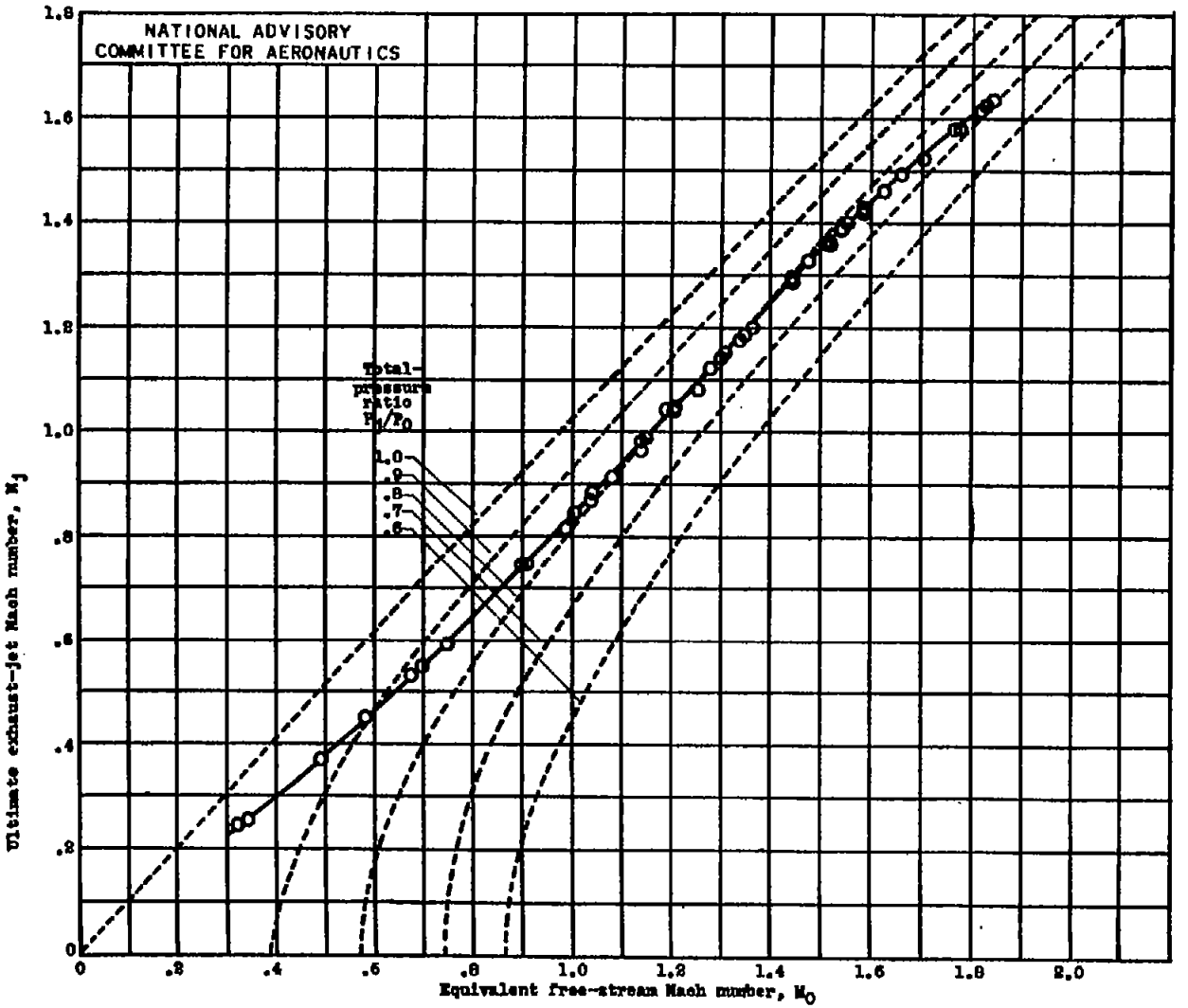

Figure 16.- Effect of equivalent free-stream Mach number M_0 and total-pressure ratio across ram jet P_j/P_0 on ultimate exhaust-jet Mach number M_j. Total-pressure ratio curves calculated for ratio of specific heats at exhaust-jet condition $\gamma_j = 1.3$ and at free-stream condition $\gamma_0 = 1.4$. 20-inch ram jet with 5-foot combustion chamber and 16.8-inch-diameter exhaust nozzle.

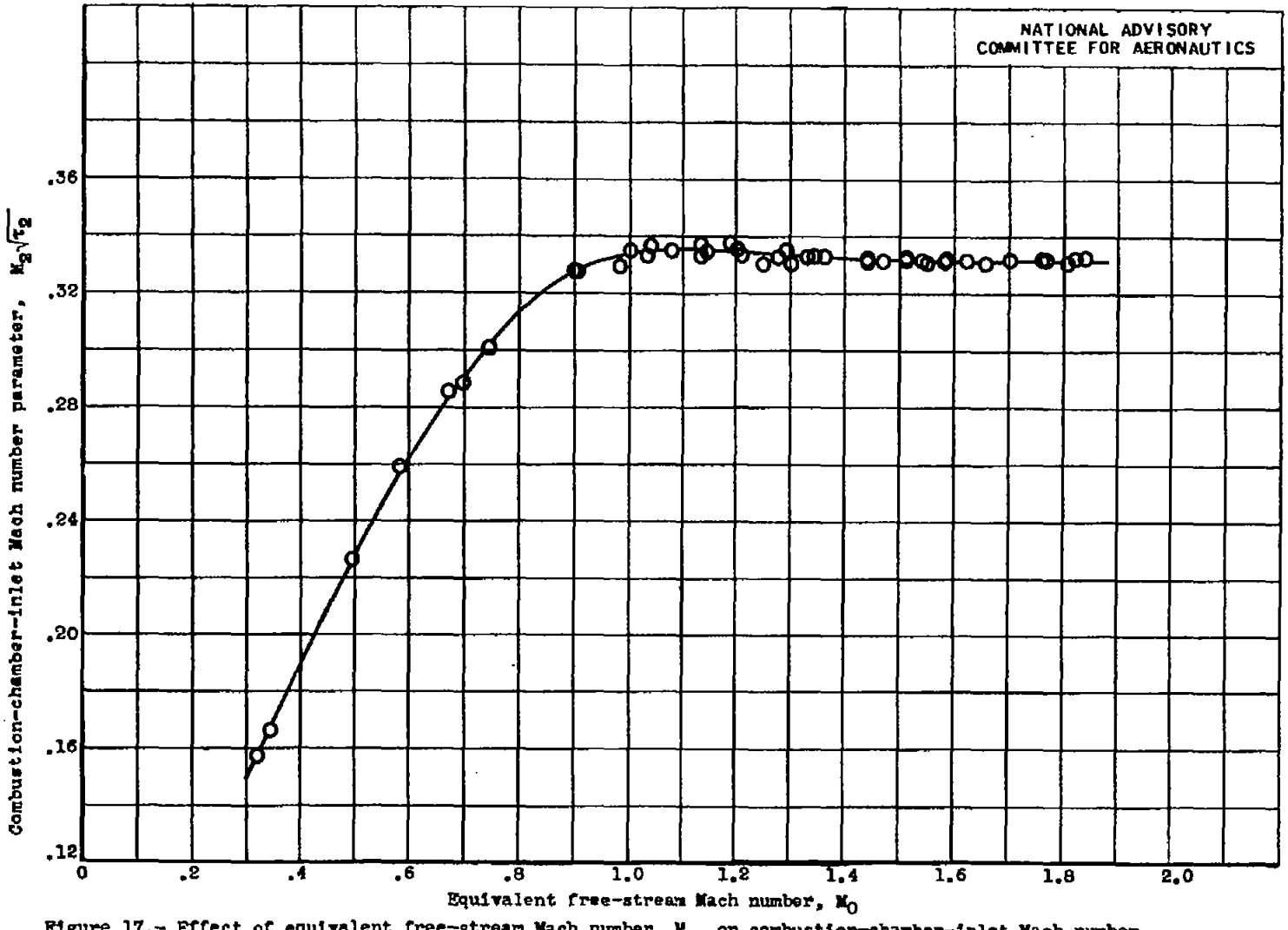

Figure 17.- Effect of equivalent free-stream Mach number M_0 on combustion-chamber-inlet Mach number parameter $M_2\sqrt{\tau_2}$. 20-inch ram jet with 5-foot combustion chamber and 16.8-inch-diameter exhaust nozzle.

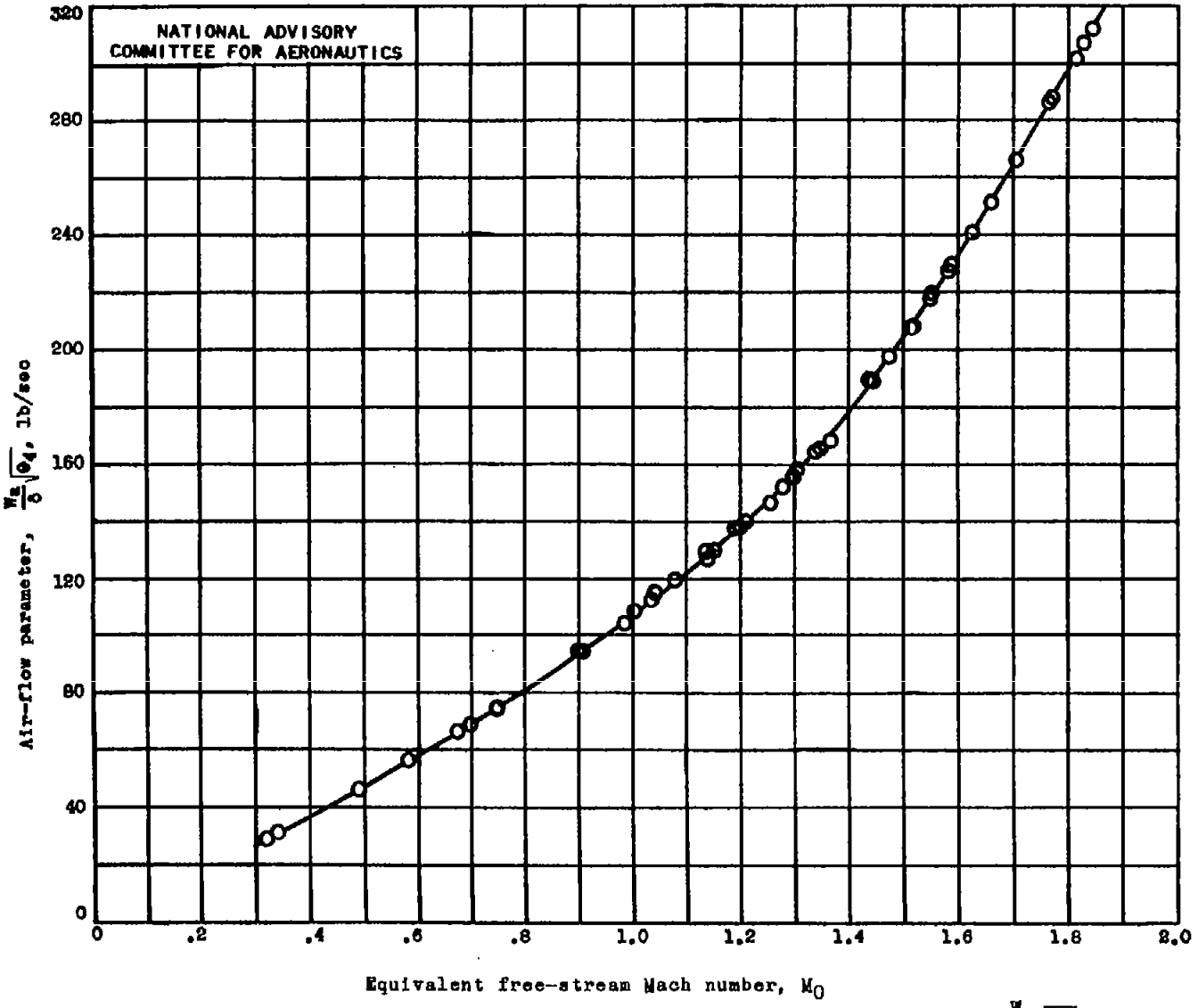

Figure 18.-Effect of equivalent free-stream Mach number M_0 on air-flow parameter $\frac{W_a\sqrt{\theta_4}}{\delta}$. 20-inch ram jet with 5-foot combustion chamber and 16.8-inch-diameter exhaust nozzle.

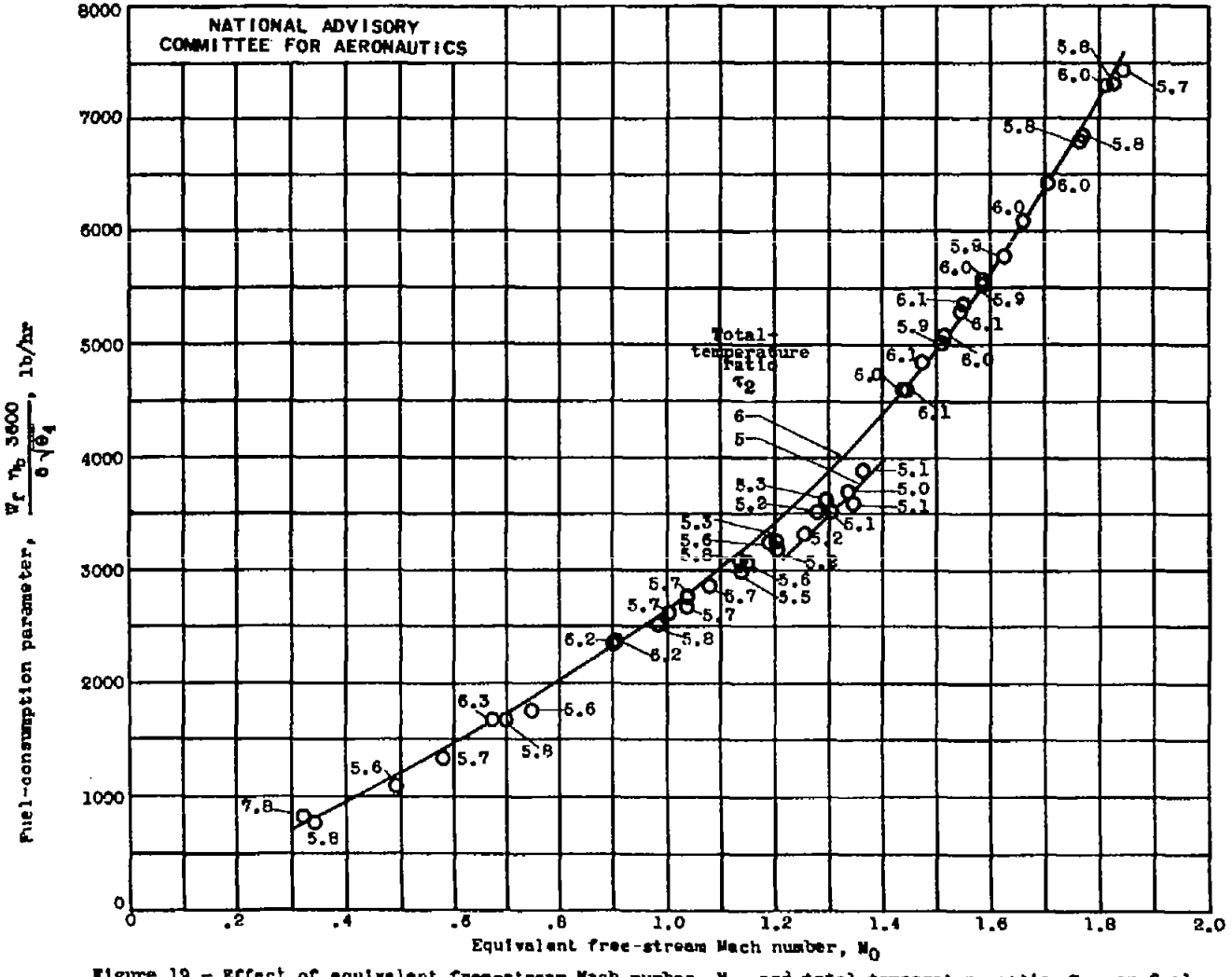

Figure 19.- Effect of equivalent free-stream Mach number M_0 and total-temperature ratio τ_2 on fuel-consumption parameter $\frac{W_f \eta_b 3600}{\delta\sqrt{\theta_4}}$. 20-inch ram jet with 5-foot combustion chamber and 16.8-inch-diameter exhaust nozzle.

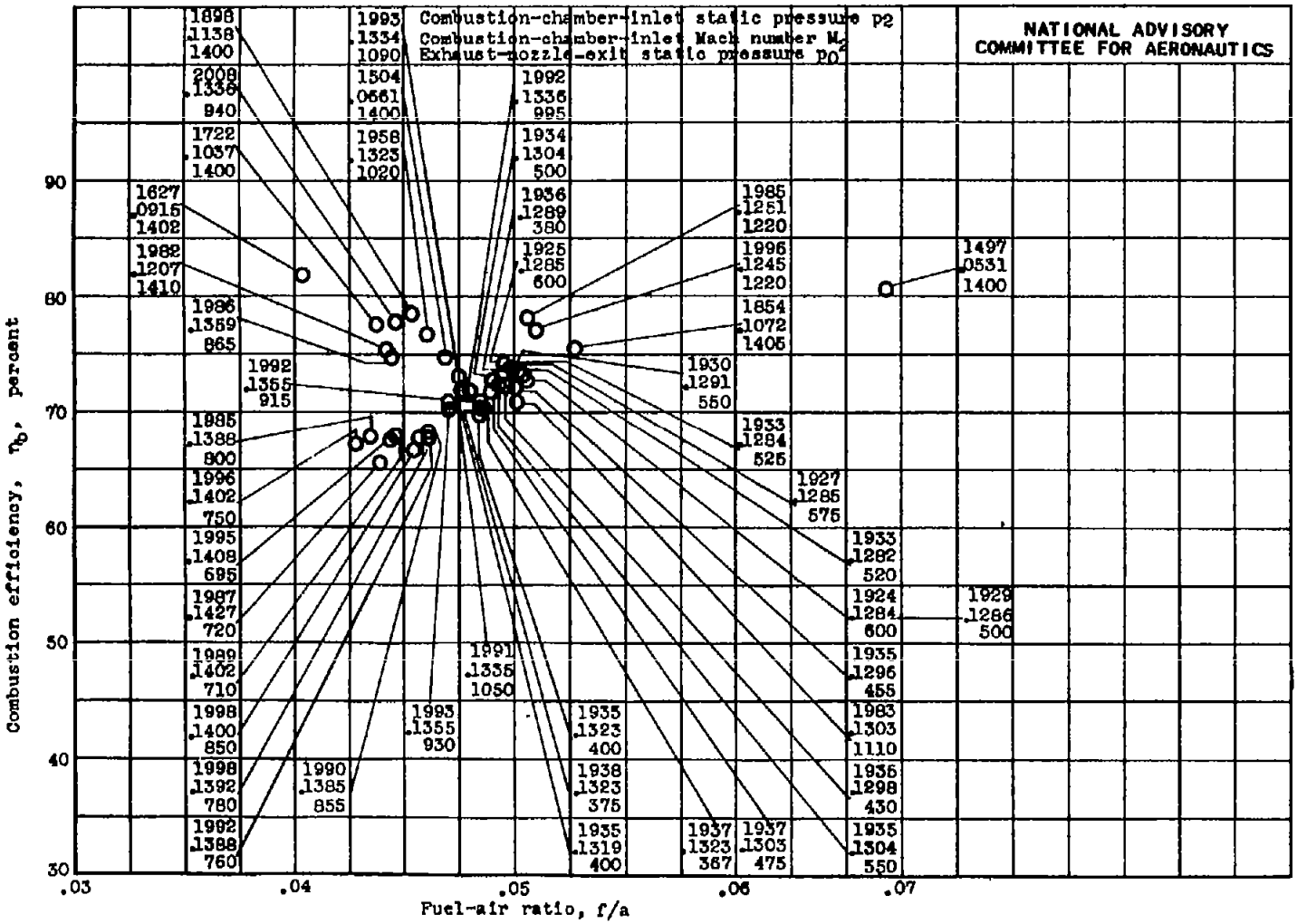

Figure 20.- Effect of fuel-air ratio f/a, combustion-chamber-inlet absolute static pressure p_2 and Mach number M_2, and combustion-chamber-exit absolute static pressure (tunnel ambient pressure) p_0 on combustion efficiency η_b. 20-inch ram jet with 5-foot combustion chamber and 16.8-inch diameter exhaust nozzle.

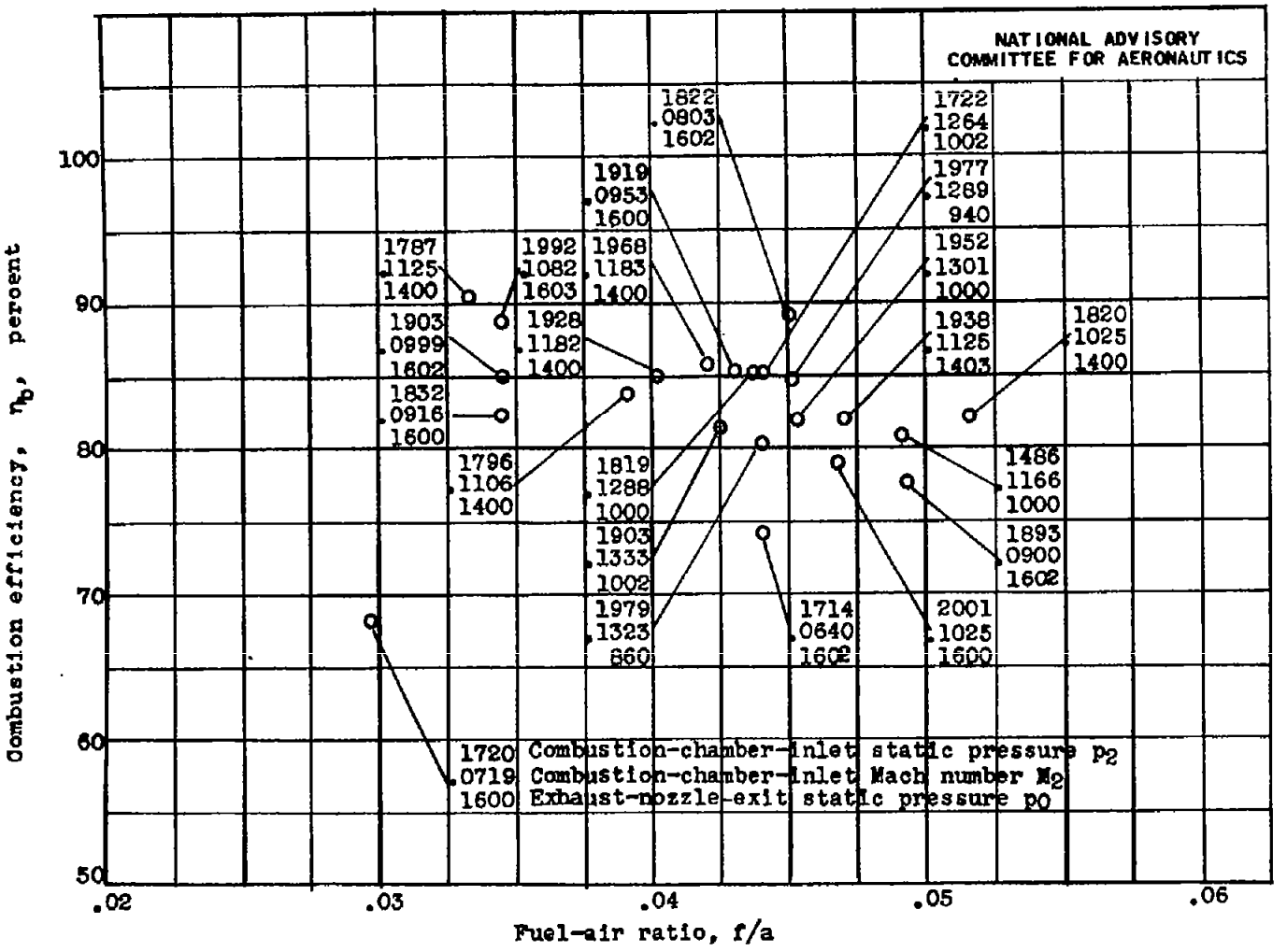

Figure 21.- Effect of fuel-air ratio f/a, combustion-chamber-inlet absolute static pressure p_2 and Mach number M_2, and combustion-chamber-exit absolute static pressure (tunnel ambient pressure) p_0 on combustion efficiency η_b. 20-inch ram jet with 12-foot combustion chamber and 16.8-inch diameter exhaust nozzle.